Chapter 6
Integration of Distribution Grid Constraints in an Event-Driven Control Strategy for Plug-in Electric Vehicles in a Multi-Aggregator Setting

Klaas De Craemer, Stijn Vandael, Bert Claessens and Geert Deconinck

Abstract In literature, several mechanisms are proposed to prevent Plug-in Electric Vehicles (PEVs) from overloading the distribution grid [1]. However, it is unclear how such technical mechanisms influence the market level control strategies of a PEV aggregator. Moreover, the presence of multiple aggregators in the same distribution grid further complicates the problem. Often, grid congestion management mechanisms are proposed to solve the potential interference between the technical and market objectives. Such methods come at the expense of additional complexity and costs, which is not beneficial for the large scale application of demand response. In our work, we investigate this problem by combining a simple low level voltage droop controller with an event driven control strategy for the coordination of charging PEVs. The approach is evaluated in different distribution grid settings, using two different market objectives for the aggregator.

6.1 Introduction

In a liberalized electricity market, aggregators are typically seen as the actors who will utilize the flexibility of PEVs. To control their PEVs, an aggregator typically determines a collective charging schedule for the fleet, based on wholesale energy

K. De Craemer · G. Deconinck (✉)
Department of Electrical Engineering (ELECTA - EnergyVille), KU Leuven, PB2445
Kasteelpark Arenberg 10, 3000 Leuven, Belgium
e-mail: geert.deconinck@esat.kuleuven.be

K. De Craemer
e-mail: klaas.decraemer@esat.kuleuven.be

S. Vandael
Department of Computer Science, KU Leuven, Celestijnenlaan 200A, 3000 Leuven, Belgium
e-mail: stijn.vandael@cs.kuleuven.be

B. Claessens
Flemish Research Institute (VITO), Boeretang 200, 2400 Mol, Belgium
e-mail: bert.claessens@vito.be

prices or its portfolio position. However, charging PEVs are physically connected to a distribution grid, which is inherently constrained by its infrastructure. To assure correct operation of the distribution grid, the Distribution System Operator (DSO) can enforce constraints by using grid congestion management mechanisms.

To integrate both aggregator and DSO objectives in the coordination of PEV charging, we identified two operation levels [2]:

- The **market operation level** entails actions with the objective of following beforehand traded volumes on the wholesale electricity markets, where trading takes place on relatively long-term scale (months, seasons) and amounts are expressed as energy quantities—usually MWh—in time slots of typically 1 h or 15 min.
- The **real-time operation level** entails the actions to comply with instantaneous consumer preferences and respect local grid constraints. Because changes and control are relatively more instantaneous and dynamic at this level, real-time operation (or technical operation) is usually expressed in terms of electrical power, e.g. kW. Granularity is in the range of minutes to seconds. At this level, fast responses are important and the number of exchanged messages will be limited.

The influence between market operation and real-time operation in coordinated charging of PEVs is often overlooked. A large part of research on integration of PEVs is aimed at optimally coordinating charging at the market operation level, facilitating larger shares of renewable energy sources or providing system-wide ancillary services. At the same time, a lot of work in literature has been carried out towards the use of PEVs to avoid distribution grid overloads or reducing losses [3, 4], objectives that are situated in the technical operation level.

However, the market and technical level can come into conflict, which typically occurs when the distribution grid is constrained or overloaded, at which point the technical objectives will intervene in the market objective(s). As market operation is overruled, consumption can deviate from what is intended by the aggregator. Multiple aggregators active in the same distribution grid further complicate this problem.

In this chapter, we analyze the influence of the real-time operation level on the market operation level by simulating both levels in a set of varying distribution grid scenarios with a single aggregator and multiple aggregators. For the market operation level, an existing event-driven market-based control (MBC) for coordinated PEV charging is used. For the real-time operation level, an optional voltage droop controller is used to mitigate local voltage limitations. In our analysis, we quantify the optimality of the aggregator's objective at the market operation level, while using droop controllers.

The contributions of this chapter can be summarized as follows:

1. Analysis of the influence of grid constraints in an event-driven control strategy for PEVs. Attention is paid to the effect of grid constraints on an aggregator's

market-level objectives, optionally with the use of a voltage droop controller to alleviate grid congestion.
2. Analysis of the influence of grid constraints in a multi-aggregator setting.

In Sect. 6.2, existing algorithms and models for both market and real-time operation levels are discussed. In Sect. 6.3, the choice of algorithm for the market operation level is detailed and motivated. Then, in Sect. 6.4, a set of relevant distribution grid scenarios is described, together with an explanation of the models and assumptions for the simulations. In Sect. 6.5, the chosen algorithms are simulated in these predefined scenarios, and the influence of real-time operation on market-level objectives is thoroughly analyzed. Finally, the same scenarios are analyzed for a multi-aggregator setting in Sect. 6.6.

6.2 Background

6.2.1 Market Level Operation

Current research regarding the optimization and coordination of clusters of Demand Response (DR) participants at the market level can roughly be divided according to the way the optimization is performed; distributed, centralized and aggregate and dispatch algorithms. This is illustrated in Fig. 6.1.

Distributed algorithms perform a significant part of the optimization process of allocating energy over the cluster at the participating devices themselves. This way, the computational complexity of finding a suitable solution is spread out over the demand response cluster, typically using an iterative process where information is communicated between the participants. However, the distributed aspect does not exclude the existence of an entity responsible for initiating or coordinating the convergence over the iterations.

One share of distributed algorithms in literature is based around distributed optimization techniques, in which a large optimization problem is divided in smaller parts that can be iteratively and independently solved [5–9]. In particular the use of gradient ascent methods and its derivatives, such as dual decomposition, are common.
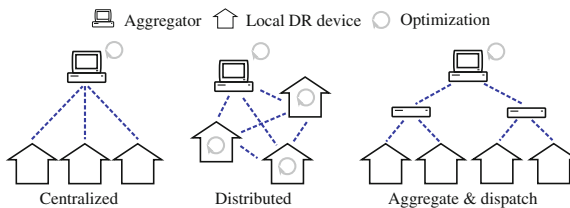

Fig. 6.1 Illustration of the three classes of algorithms and coordination for DR at the market-level

Centralized algorithms are entirely the opposite. A central actor collects information that is sent to it from the DR devices. This information can consist of individual constraints and deadlines or comfort settings. Using the collected knowledge, and possibly including its own additional information such as predictions or stochastic functions, the central coordinator can perform a single optimization that returns an optimal schedule satisfying all the constraints at once. Inherently, this makes centralized algorithms the least scalable, as the optimization process quickly becomes intractable with an increasing number of participating devices. Furthermore, the communication towards and from a single point poses a potential bottleneck. Several solutions are proposed that help to overcome the tractability issue [10, 11]. In [12], focus is on ensuring that vehicle owners truthfully report their value for receiving electricity, willingness to wait and maximum charging rate. Owners could misreport their availability, for example by unplugging early or plugging in the vehicle some time after arrival to try and get a better price.

Inbetween distributed and centralized mechanisms are the **aggregate and dispatch algorithms**. They decouple the optimization of the objective and the dispatch of its outcome, thus alternatively the term 'dispatching mechanism' is equally fitting. An aggregate & dispatch mechanism allows information (such as constraints) from and to the central entity to be aggregated, reducing the complexity of the optimization and improving scalability, but carrying certain compromises or constraints regarding the optimality of the results. The work of [13–15] follows this idea.

While distributed and centralized algorithms can determine an optimal DR schedule given the device's constraints, market data,… they carry some disadvantages regarding computation times, complexity or communication. Aggregate and dispatch mechanisms are a compromise allowing for a scalable and low-cost implementation, at a limited loss in optimality [16]. In our work, we have chosen to work with one aggregate & dispatch algorithm in particular, MBC. We will discuss this method in more detail in Sect. 6.3.

6.2.2 Real-Time Level and Grid Congestion

As the electricity grid cannot get physically congested, the term *grid congestion* refers to a situation where the demand for active power exceeds the nominal power transfer capabilities of the grid [17]. Grid congestion can be mapped to the violation of one or more constraints at its connection points. In the context of this chapter, these will mainly be in the form of power quality problems in distribution grids, and can be attributed to the resistive and unbalanced nature of distribution grids.

6.2.2.1 Grid Congestion Metrics

The European EN 50160 standard, "Voltage characteristics of electricity supplied by public distribution systems" [18], describes, among others, the following important specifications:

- Over- and undervoltage: "The European EN 50160 standard specifies that the 10 min mean RMS voltage deviation should not exceed ± 10 %, measured on a weekly base. For undervoltages, a wider range is allowed in the measurement procedure: −15 to −10 % during maximum 5 % of the week."
- Voltage dip: EN 50160 allows 1,000 voltage dips per year, during which the voltage drops at most to 85 % of its nominal value, for a duration of less than 1 min. Interruptions, defined as lasting less than 180 s, should occur less than 500 times/year.
- Voltage unbalance factor (VUF): When magnitudes of phases or line voltages and the phase angles are different from balanced conditions. "The European EN 50160 standard specifies that the 10 min mean RMS value of the voltage unbalance factor should be below 2 % for 95 % of time, measured on a weekly base." Different ways to compute the VUF exist, and here we will use *True VUF* as shown below. More information on the definitions and calculation of VUF can be found in [19].

$$\text{True VUF} = \frac{\text{negative voltage sequence component } V_n}{\text{positive voltage sequence component } V_p}$$

$$\text{with } V_p = \frac{V_{ab} + aV_{bc} + a^2V_{ca}}{3} \tag{6.1}$$

$$\text{and } V_p = \frac{V_{ab} + aV_{bc} + a^2V_{ca}}{3}$$

- Harmonics: Caused by the power electronics inside converters such as found inside vehicle chargers or photovoltaic (PV) inverters. Harmonics will not be looked into here, but the use of power electronics such as found inside PEV chargers can create problematic harmonics [20].

6.2.2.2 Congestion Mitigation

A distribution system operator, faced with grid congestion problems, can opt for a number of mitigating strategies.

- **Reactive power and voltage control** to increase the (local) transfer capacity. This is already used in wind generators connected to the medium voltage network. In distribution grids, reactive power and voltage control can be achieved through the use of tap changers and capacitor banks, and their switching is planned using load forecasts. For example, [21] optimizes to limit switching of such devices.
- **Coordinating the power flow** [17] throughput via shifting or curtailment of demand, possible through the implementation of demand response, or through the mandated implementation of voltage droop control.

- **Increasing the transfer capacity** of the local grid by replacing or upgrading equipment (adding or replacing cables, installing a bigger transformer…). While this option is attractive because it limits the involvement of the DSO (retain 'passive' role, no forecasts …), the cost of this option can be substantial and thus only considered when other solutions are exhausted or deemed infeasible.

The first option is already used today. However, in practical operation, low voltage-grid tap changers are usually off-load types and barely used [22]. Tap positions are calibrated and changed only in case of network extension or modification [23]. Automated and remotely controllable on-load tap changers (OLTC) exist, but their use in distribution grids is still reserved to a few test cases [24], due to costs.

The third option is technically attractive for DSOs, since it fits within a predominantly off-line role of installation, maintenance and asset management at the distribution network level.

Adding parallel cables to or upgrading existing lines by using new cables with higher cross sections is considered a straightforward solution [23]. No additional tasks such as day-to-day load forecasting, extensive state estimation and monitoring are required. The high investment costs will likely reserve this to some corner-cases.

In the remainder of this chapter, congestion management will refer to the use of the second option; the coordination of active power demand at congested grid locations. In the light of the real-time and market operation levels, we will now discuss the use of voltage droop control and grid congestion management mechanisms.

6.2.2.3 Voltage Droop Control

As mentioned, lines in distribution grids behave resistively rather than inductively. This causes voltage deviations along the line when large amounts of active power are drawn from or injected into the grid. To avoid such effects, large-scale PV installations in some countries are now required to be able to provide grid services to the DSO. Similarly, small PV installations are required to respond to overfrequency and overvoltage by limiting injected power or temporarily disconnecting [25, 26].

But PV output is determined by the uncontrollable radiation of the sun, whereas charging rates of PEVs can be varied and shifted arbitrarily in time. Thus, in addition to the coordination at the market level, a fast-acting grid-supportive behavior similar as used in PV installations can be implemented inside a charger [27–29]. It is not unthinkable that the use of automatic voltage control for Electric Vehicle Supply Equipment (EVSE) becomes mandatory as well once their impact reaches a significant quantity.

Nonetheless, a droop control scheme is robust and easy to implement because it only requires the measurement of voltages and a way to adjust local active or
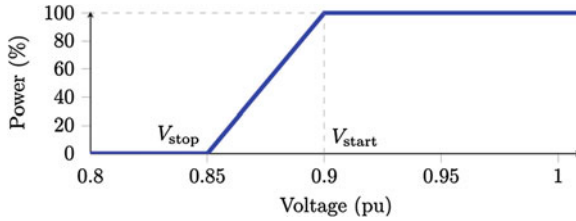
Fig. 6.2 Example voltage droop control characteristic for PEV chargers

reactive power settings. No communication with a central entity is needed. An example of a voltage droop curve for a PEV charger is shown in Fig. 6.2. When the voltage at its connection point drops below 0.9 per unit (pu), power is linearly reduced until 0.85 pu, where charging is completely halted.

On the downside, activation of the droop will almost certainly conflict with market level coordination [30] (Sect. 5.2.4). For example, at some point the fleet manager would send its optimal power set-points or an equilibrium priority to the vehicle agents. But due to local grid problems the EVSE is forced to reduce power. The result is that, even if the real resulting power setting is communicated back to the fleet manager, the deviation holds a disparity from the original optimal market level energy plan. The resulting energy shortfall (negative imbalance) may result in a penalty for the fleet manager.

6.2.2.4 Advanced Congestion Management Mechanisms

The task of a grid congestion management mechanism is to limit the managed loads to the capacity of the distribution grid assets at any time, especially in the presence of multiple competing actors with different objectives. This can be achieved by adding a network cost or penalty for the use of the network during certain times of the day. In [17], algorithms for congestion management are classified according to strategy.

- **Distribution grid capacity market**: In this mechanism, the aggregators involved will start by optimizing the schedule for their PEVs in absence of a network tariff. The schedule is sent to the DSO, which evaluates whether the network constraints are met. If not, the aggregators will receive a price that reflects congestion at each node in the network and are requested to update their schedule.

  The procedure is then repeated until convergence, at which point the network tariff and charging schedules are fixed. As the mechanism is essentially the same as dual decomposition, the use of non-strict convex objective functions can cause problems. In [31, 32], this method is used.

  A capacity market would be complex to implement and the iterations add a lot of computational burden. The DSO could be offloaded by externalizing the

process into a separate capacity market, in which it still has to provide measured and estimated power.

- **Advance capacity allocation system**: The idea behind this mechanism is that the DSO pre-allocates grid capacity at each transformer or line to the aggregators, based on the free capacity remaining at each line or transformer, after inelastic load (mainly household consumption) has been accounted for. The allocation between aggregators would be based on auctioning of this free capacity.

    While relatively straightforward, there are some drawbacks to this method. First of all, the DSO needs to map all its customers' connection points to their respective aggregator. Secondly, there is no way to incorporate the time-dependency of demand; if an aggregator bids for the capacity during certain time, that bid depends on what was allocated before and after that time-period. An iterative approach would solve this, but also increases complexity again.

- **Dynamic grid tariff**: In this case, a time-varying location-dependent grid tariff is determined by the DSO beforehand, based on expected consumption levels at each node in the grid. Predicting loads and estimating price-sensitivity is entirely the responsibility of the DSO. Once the tariffs are published to the aggregators, the latter integrate them into their scheduling. In case of severe deviations from the expected value, the DSO may resort to controlled interruptions in real-time, which in turn also holds a risk for the aggregators. The work of [33] uses this approach. The biggest drawback consists of the high complexity of the problem that needs to be solved by the DSO (predictions, load flow calculations…), let alone when the stochastic properties of inevitable uncertainties are taken into account.

The work of [34] (p. 97) provides an overview and comparison of these 3 types of mechanisms. While all of the mechanisms should lead to the same optimal PEV charging profile, the complexity involved limits their practical implementation. It is also not clear how deviations during the course of the day should be handled, which will inevitably occur as the algorithms are based on the use of allocations in time slots (e.g. 15 min in [32]), besides the last-resort of DSO-controlled interruptions.

In [34] (p. 100) the use of a simpler proxy tariff is proposed, such as a historical *ToU* or real-time tariff, as a compromise. Unfortunately, following simulations, the conclusion suggested that the use of proxy tariffs does not necessarily reduce system peak load, leads to higher costs (approx. +20 %) and distorts the economic signal of the electricity price.

6.3 Market-Level Operation: Market-Based Control for PEVs

The concept of MBC is rooted in the theory of microeconomics, wherein economic activity is modeled as an interaction of individual parties pursuing their private interests [35] (Chap. 4). The market mechanisms that apply provide a way to incentive the parties, referred to as economic agents, to behave in a certain way.

In [36], appliances in a DR cluster are represented by software agents in a multi-agent system (MAS). They have control over one or more local processes (e.g. heating of water or charging of a PEV's battery), but compete for resources (electric power) on an equilibrium market with other agents.

6.3.1 Architecture

The MBC system has been used in a number of field tests and is commercially known as PowerMatcher. The clearing of the market in [36, 37] is operated on a periodic basis, e.g. a time slot length of 15 min, or using events, and is implemented in a hierarchical, tree-like manner [35], as illustrated by Fig. 6.3a.

At the root of the tree is an auctioneer agent, directly connected to a number of *concentrator agents*. The *auctioneer agent* is a special type of concentrator agent and is responsible for the price setting process, just as in the Walrasian auctions. The concentrator agents lower in the tree aggregate the demand functions of their child agents. Because a uniform interface is used between the levels, an unlimited number of such aggregation levels can be used. Eventually, at the bottom of the tree, we find the *device agents* themselves.

The device agents assemble *demand functions* representing their willingness to pay and consume, taking into account the specific constraints of the controlled device. Demand functions are sent upwards and an auctioneer agent performs a matching process with producing agents. An equilibrium price is communicated back to the agents, that start consuming or producing at the equilibrium level.

If equilibrium prices are regarded as a pure control signal, so that there is no direct link to the cost of energy, the MAS MBC mechanism can be viewed as a dispatching method for the aggregator's business case. In such scenario, the demand function data is regarded as input for a scheduling algorithm, and the equilibrium price (or better, *equilibrium priority*) as a level to steer the cluster towards its outcome.

6.3.1.1 Demand Functions for PEV Device Agents

Representative demand functions can be built using various means, but in case of PEVs, a straightforward way is by combining each agent i's requested energy $^iE_{req}$, time till departure $^i\Delta t_{dep}$ and maximum charging power $^iP_{max}$ to create a sloped curve $^iP_{dem}$, as shown below each PEV in Fig. 6.3a and also in Fig. 6.3b. In case there is not enough time left to receive the requested energy ($t_{critical}$ occurs before the current time), an inflexible demand function can be used, so that charging happens at maximum power regardless of the control signal.
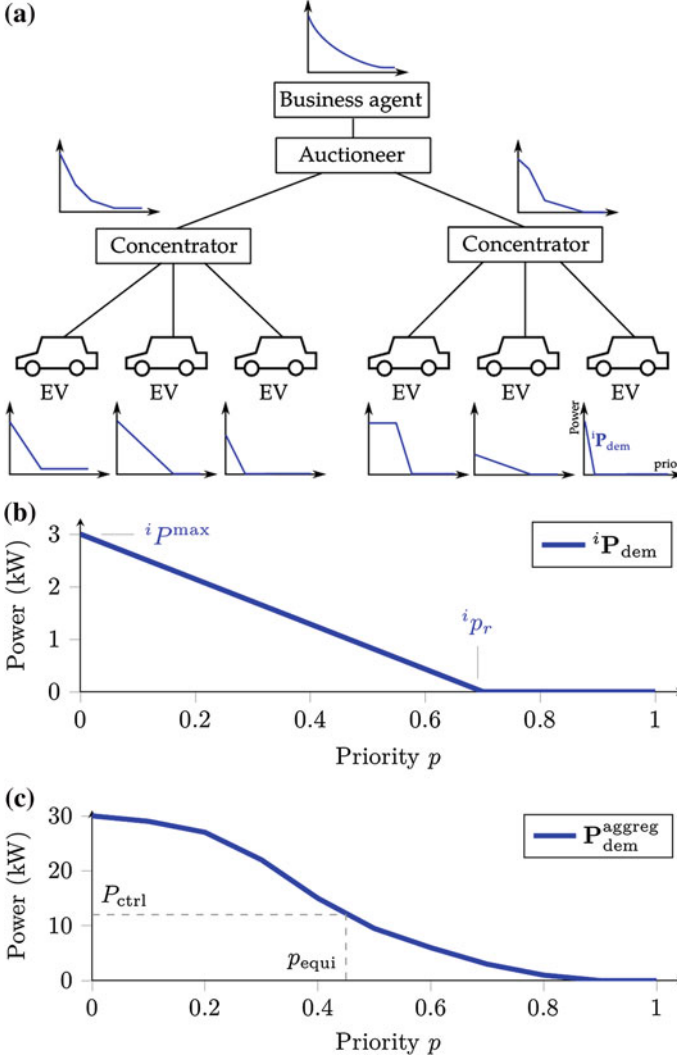
Fig. 6.3 Overview of the control structure in MAS MBC in (**a**). Device agents, pictured as charging PEVs, send demand functions $^{i}P_{\text{dem}}$, shown in (**b**), upwards. After aggregation of the individual demand functions, equilibrium priority p_{equi} is determined, shown in (**c**), and sent back to the agents

$$^{i}P_{\text{dem}} = f\left(^{i}E_{\text{req}}, ^{i}\Delta t_{\text{dep}}, ^{i}P_{\text{max}}\right) \tag{6.2}$$

$$^{i}t_{\text{critical}} = t| ^{i}E_{\text{req}} = ^{i}P_{\text{max}}\,^{i}\Delta t_{\text{dep}} \tag{6.3}$$

A detailed description of building demand functions for PEVs in this context can be found in [2, 16].

6.3.1.2 Concentrator Agents and Aggregation

At the concentrator agents, the individual demand functions of n agents are aggregated into a single curve $P_{\text{dem}}^{\text{aggreg}}$, shown in Fig. 6.3c. At the auctioneer agent, this aggregated curve is used to find the equilibrium priority p_{equi} that corresponds to a desired power setting P_{ctrl} for the DR cluster.

$$P_{\text{dem}}^{\text{aggreg}} = \sum_{i=1}^{n} {}^{i}P_{\text{dem}} \tag{6.4}$$

$$p_{\text{equi}} = P_{\text{dem}}^{\text{aggreg}}|P_{\text{ctrl}} \tag{6.5}$$

The value for P_{ctrl} has to be determined by the business agent.

6.3.2 MAS MBC Advantages and Drawbacks

Using a multi-agent market based control system (MAS MBC) for demand response, as exemplified by the PowerMatcher, offers several benefits.

- Scalability: In a centralized system, the central entity has to deal with all incoming and outgoing messages, $O(n)$, quickly creating a communication bottleneck. Because of the aggregation on multiple levels in the PowerMatcher, the amount of messages that have to be dealt with per agent can be reduced to $O(\log n)$.
- Low complexity: The construction of demand function data and the matching process itself is straightforward, and is not based on any model. Determining a demand function for a device can be done during its development.
- Openness: Any kind of device can be integrated in the cluster, since operation only depends on the exchange of demand functions and price. Devices without flexibility are represented by an inelastic demand function.
- Privacy: Since demand functions are aggregated there is no central entity that collects all information. Furthermore, the physical processes of devices, bidding strategy and motives of users are all abstracted through their demand functions.

As indicated before, the use of an aggregated model at the auctioneer agent and a heuristic to build the PEV's demand functions will lead to a suboptimal solution. However, a more significant shortcoming compared to other methods presented in this chapter, is the lack of look-ahead functionality.

6.3.3 Addition of Scheduling Functionality and Control Objectives

For loads that can store electric energy, such as PEVs, an *energy constraints graph* can be used to capture the available flexibility over a certain time horizon. This is introduced in the work of [16]. For each PEV i, two vectors ${}^{i}\boldsymbol{E}_{\max}$ and ${}^{i}\boldsymbol{E}_{\min}$ are added to the information ${}^{i}P_{\mathrm{dem}}$ sent from device agents to auctioneer agent.

The vector ${}^{i}\boldsymbol{E}_{\max}$ is the energy path of a PEV agent i, if it were to start charging immediately at maximum power and then (at t_{idle}) stay idle until its departure time t_{dep}. On the other hand, ${}^{i}\boldsymbol{E}_{\min}$ represents the case when charging is postponed as long as possible (up to t_{critical}). This is expressed in the equations below and illustrated in Fig. 6.4a. All area in between ${}^{i}\boldsymbol{E}_{\max}$ and ${}^{i}\boldsymbol{E}_{\min}$ represents the flexibility of the charging process.

$$
{}^{i}\boldsymbol{E}_{\max} = \left\{ {}^{i}E_{\max}(t) \mid {}^{i}E_{\max}(t) = \min\left(t\,{}^{i}P_{\max}, {}^{i}E_{\mathrm{req}}\right) \forall t \in \left\{0, 1, \ldots {}^{i}\Delta t_{\mathrm{dep}}\right\}\right\}
$$
$$
{}^{i}\boldsymbol{E}_{\min} = \left\{ {}^{i}E_{\min}(t) \mid {}^{i}E_{\min}(t) = \max\left({}^{i}E_{\mathrm{req}} - \left({}^{i}\Delta t_{\mathrm{dep}} - t\right){}^{i}P_{\max}, 0\right) \forall t \in \left\{0, 1, \ldots {}^{i}\Delta t_{\mathrm{dep}}\right\}\right\}
$$
$$
\tag{6.6}
$$

To represent the battery constraints of an entire PEV fleet of n vehicles, the individual constraints are aggregated into collective battery constraints $\boldsymbol{E}_{\max}^{\mathrm{aggreg}}$ and $\boldsymbol{E}_{\min}^{\mathrm{aggreg}}$, at the intermediate agents and the auctioneer agent. The auctioneer agent can now use the collective energy constraints to determine an optimal path $\boldsymbol{E}_{\mathrm{opt}}$ over the horizon t_{horizon}, according to some objective function C:

$$
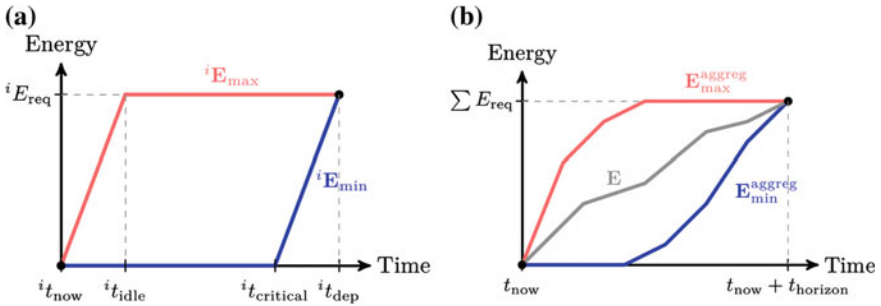\boldsymbol{E}_{\mathrm{opt}} = \underset{\boldsymbol{E}}{\arg\min}\, C(\boldsymbol{E}) \tag{6.7}
$$

Fig. 6.4 **a** Energy constraints graph for a single vehicle i, and **b** aggregated energy constraints graph and some scheduled path $\boldsymbol{E}$ through it

with: $E = \{E_t$ $\forall t \in \{0, 1, \ldots, t_{\text{horizon}}\}\}$,

subject to: $P_t \leq P_t^{\text{limit}}$ $\forall t \in \{0, 1, \ldots, t_{\text{horizon}}\}$

$E_{\text{min,t}}^{\text{aggreg}} \leq E_t \leq E_{\text{max,t}}^{\text{aggreg}}$ $\forall t \in \{0, 1, \ldots, t_{\text{horizon}}\}$

$E_{t+1} = E_t + P_t \Delta t$ $\forall t \in \{0, 1, \ldots, t_{\text{horizon}} - 1\}$

Here E_t is the collective energy of the cluster at time t, and P_t is the power consumed by the cluster during time t to Δt. Any objective $C(\boldsymbol{E})$ can be used to determine a path for the PEV cluster, and in Sect. 6.4.1, two objectives will be discussed.

6.3.4 Event-Driven Approach

Communication takes on an important role in demand side management of PEVs. Charging requirements and constraints need to be communicated to an aggregator, while aggregators need to send control signals back to PEVs in order to steer their charging power towards cluster-wide goals.

In terms of integrating charge coordination algorithms into a realistic "real-world" environment, two challenges are identified: continuous coordination, and messaging limitations.

The first challenge is the need for continuous coordination of the charging process. In energy markets, charging only needs to be optimized in terms of energy volume per hour. However, vehicles arrive and depart continuously, and will want to start charging or depart at asynchronous times.

This means that, ideally, control and coordination actions should also commence immediately, especially for fast-charging applications, and allow for quickly altering the fleet's behavior if the need arises. Consequently, charging needs to be coordinated at two levels: a market level, where time is divided in time slots, and a real-time, event-driven level that is focused on responsiveness. This division applied to the MBC architecture is illustrated in Fig. 6.5.

In this case, event-based interaction allows the PEVs and aggregator to quickly respond to changes in setpoint or in flexibility. If a situation occurs where vehicles have to slow down charging due to distribution grid constraints, the aggregator is informed and will try to use flexibility from other vehicles that do not experience such problems.

The second challenge is related to the exchange of messages between PEVs and an aggregator. In reality, the underlying infrastructure places constraints on the communication, pertaining to packet delays, link reliability or maximum through-put. In the latter case, the exchange of messages should be limited by the coordination mechanism, which is done by caching information from and to the PEVs. More details on the event-driven implementation can be found in [2].

Fig. 6.5 MAS MBC
architecture with dual
coordination. The real-time
part is event-driven, while the
market operator works in
discrete time intervals (time
slots)
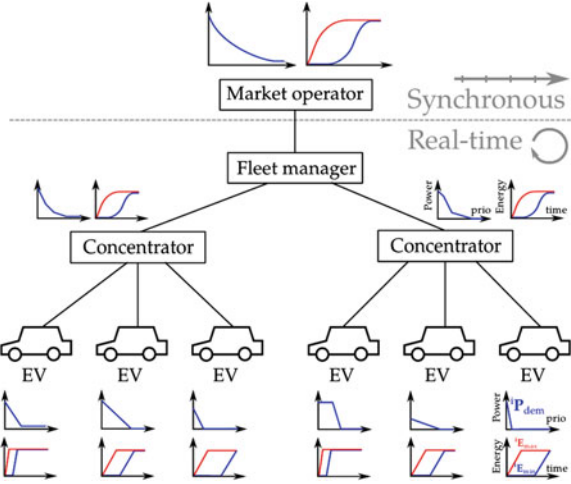
6.4 Simulation Objectives and Models

We want to investigate the situation where an aggregator coordinates a cluster of
PEVs based on market-level objectives, but a large part or all of the vehicles are
situated inside a weak and constrained grid topology. How effective is the use of a
voltage droop controller in eliminating or reducing grid congestion problems? To
what degree do the technical objectives impact the aggregator's business case?

To answer these questions, a simulation framework was developed; a Java-based
part allows to model the interaction between the agents, while the market-level
optimization is performed in Matlab using CPLEX. To simulate the effects on the
voltages in a distribution grid, a Matlab-based backward-forward sweep load flow
solver developed at our research group was also integrated in the framework.

Besides a framework, several models and datasets are required to properly
represent the actors and their behavior. In this section, we describe the driving
profiles and model for the PEVs, the wind prediction and generation, and the
household loads present in the distribution grids.

6.4.1 Aggregator Market-Level Objectives

Two market-level objectives for the auctioneer agent are considered:

- *Time-of-Use (ToU)*, where the aggregator's goal is to minimize the cost of
  charging a cluster of vehicles, based on a time-varying tariff p_t, and using a
  Linear Program (LP) optimization:

$$E_{\text{opt}} = \underset{E}{\text{argmin}} \sum_{t=0}^{t_{\text{horizon}}} C(E_t) \quad \text{with} \quad C(E_t) = p_t E_t \tag{6.8}$$

Because this is a linear objective, a sharp on-off control behavior can be expected.

- *Portfolio balancing*, where the goal of the aggregator is to use the flexibility of a fleet of PEVs to limit his portfolio's wind generation exposure to the imbalance markets. This means finding an optimal energy trajectory for the PEVs, E_{PEV}, over a horizon, such that the difference between short-term wind prediction E_{wind} and day-ahead nomination E_{nomin} is minimized:

$$E_{\text{opt}} = \underset{E}{\text{argmin}} \sum_{t=0}^{t_{\text{horiz}}} \left(E_{\text{PEV},t} + E_{\text{wind,t}} + \frac{1}{4} E_{\text{nomin},t/4} \right)^2 \tag{6.9}$$

In this specific case, the day-ahead nominations are required to be supplied on an hourly-basis, while the short-term wind predictions are on known a quarterly basis, 15 min ahead, and with a horizon of 24 h. The control variables of the PEVs can be on an arbitrary time basis.

Thus, as more accurate wind predictions become available after the nomination, the optimization will try to use the vehicles to limit the difference, and, due to the quadratic term, favor to spread out remaining imbalance in time (Fig. 6.6).

6.4.2 PEV Model

The model of the PEVs (hybrid plug-in or full electric) in the simulations consists of two main parts: a battery model and a usage or driving profile.

Fig. 6.6 Illustration of the balancing objective
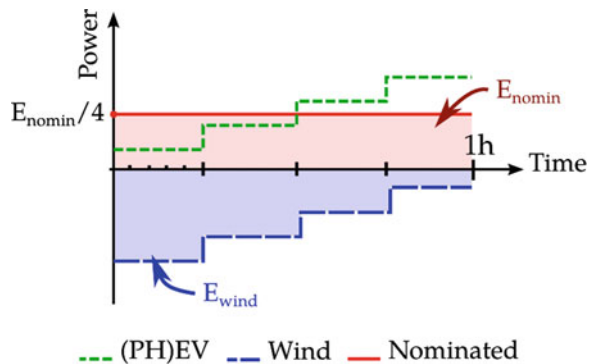
6.4.2.1 Battery and Charging

In literature, a great deal of research has been done on the characterization and use of batteries for electric drive-train applications. The purpose of the envisaged model for the simulations in this context does not include aspects such as aging and depreciation costs, and are subsequently left out in favor of a simple first order approximation of the storage capacity of the battery.

In reality though, the maximum charging current has to decrease before the battery reaches a state of charge (SOC) of 100 %, to avoid damaging the cells. Here, the charging and discharging process in the PEV is simplified to a constant power behavior, and the capacity is chosen such that it corresponds to a depth of discharge (DOD) of 83 %. This is a valid consumption, as the SOC of existing PEVs is also kept within a certain DOD to extend battery life. Summarized, all vehicle instances are equipped with the same usable battery content of 20 kWh. Technically speaking, 20 kWh would then represent a PEV with a total battery capacity of around 24 kWh.

Technical constraints in (European) residential installations limit charging power to around 3.3 kW (corresponding to 16 A at 230 V and 10 % allowed voltage deviation) or 6.6 kW (32 A). In fact, to avoid problems due to inadequate wiring or installations, some car manufacturers only allow the 3.3 kW power level when the vehicle is plugged into a so-called dedicated wall-box. Charging through standard outlets is then typically limited to 2–2.5 kW. In the battery model used here, charging takes place at a variable power level between 0 and 3.3 kW. This may seem to be a slow charging rate, but because of the long standstill times at home, the need for higher charging rates at home is not critical [38].

Also assumed that vehicles want their battery fully charged by departure, as this is the worst case and also more convenient for drivers, not having to enter an expected distance. Vehicle-to-grid scenarios were not considered.

6.4.2.2 Driving Profiles

To complete the PEV model, data about the state of the vehicle during the day (idle at home, driving, unavailable,…) and the energy consumption while driving is required.

In the work of [39], the results of the 3rd Flemish Mobility Study (OVG3) were analyzed. The latter was commissioned by the Flemish government and looks at the transportation behavior of 8,800 drivers during September 2007 and 2008. Recorded data includes the number of trips each day, distances, motives, departure times, … From this, synthetic availability profiles were prepared that can be used in simulations. An example for 2,500 vehicles is shown in Fig. 6.7, where the number of vehicles that is at home, driving or at work over the course of 7 days is plotted. It can be seen that fleet behavior is very periodic and therefore predictable.

Vehicles will only charge at home, so that the amount of energy needed reflects a worst-case scenario for the distribution grid.
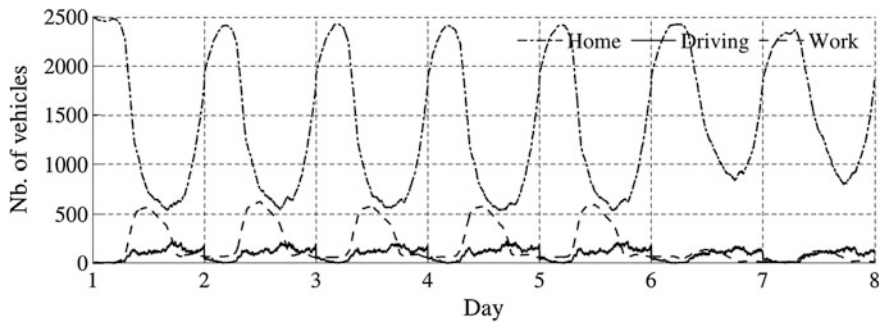
Fig. 6.7 Illustration of the used vehicle availability profiles, cumulative for 2,500 vehicles, over 7 days

For the energy consumption model, required power during acceleration and braking (related to vehicle size, aerodynamics and driver habits) has to be added on top of auxiliaries such as lighting, heating, wipers etc. More information can be found in [30] (Chap. 2), and [39, 40]. From [39], an average driving speed of 42 km/h is combined with an energy consumption of 250 Wh/km.

These numbers result in a theoretical range of 80 km for each simulated vehicle. Figure 6.8 shows the cumulative distribution of the SOC of the battery at arrival time, after a simulation with 1,000 vehicles and over 7 days. From the figure, half of the arrivals happened with a battery of almost 80 % SOC or more. However, for 6.8 % of the simulated trips, 20 kWh was insufficient. Simply increasing the usable battery size to 24 or 26 kWh does not eliminate these occurrences, so these trips are out of range for the average battery electric vehicle (BEV). It will therefore be assumed that these drivers are using a plug-in hybrid electric vehicle (PHEV) to complete their journey.
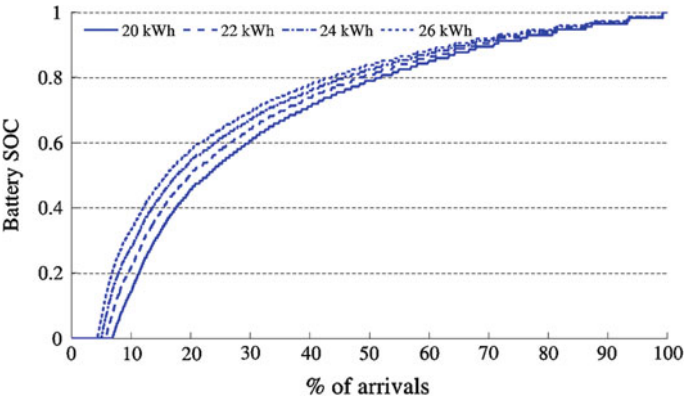

Fig. 6.8 Effect of simulated battery size on SOC at vehicle arrival, for different usable battery contents, obtained for a set of 1,000 vehicles over 7 days

6.4.3 Wind Energy Generation and Predictions

In one objective, renewable energy production from wind turbines is taken into account. For several locations in the Netherlands, both wind speed measurements and predictions are available. The wind speed predictions were calculated by the *Aanbodvoorspeller Duurzame Energie* (AVDE) at ECN [41, 42] and translated to the correct height of the turbine, as winds aloft generally have a higher velocity than winds at ground level.

The resulting wind speed then has to be put alongside the turbine's specified output power. For the turbine specifications, one type from manufacturer Nordex is used, the 2.5 MW peak N80/2500 [43].

Since the available wind speed data consists of predictions that have a horizon of 48 h, and are updated every 6 h, the most accurate predictions that can be submitted for nomination are those generated at 12h00 the day before.

6.4.4 Household Consumption

To be able to simulate the effects on voltage quality in a distribution grid, realistic household consumption profiles are required. Synthetic aggregated profiles, available from the local regulator and used by energy retailers to estimate their customers' consumption, are too generic. In the 'Linear' smart grid project [44], measurements at 100 households were performed over the course of a year, with a resolution of 15 min. When more profiles are needed the available set is rotated. An illustration of 20 of the used profiles is plotted in Fig. 6.9.

It can also be observed that there is a high simultaneity between households consumption in the evening and the arrival of PEVs.

6.4.5 Weak Grid Topology and Agent Architecture

When investigating the effects of coordinated charging on the state of the distribution grid and vice versa, it makes sense to focus on weak grid configurations, where problems are more likely to occur. The question then arises what specific topology should be used as grid model. We are focusing on the grid situation in Belgium, but from discussions with experts, information on the current state of distribution grids seems to be lacking. During planning and deployment of new grid segments, DSOs selected appropriate values for the cable sizes and lengths, and individual connection points were spaced out evenly over the phases. Decades later, sections have been added, reconfigured, new connections points have been attached to "random" phases, etc. This makes the occurrence of virtually any situation possible in practice and with the increasing share of PV installations on
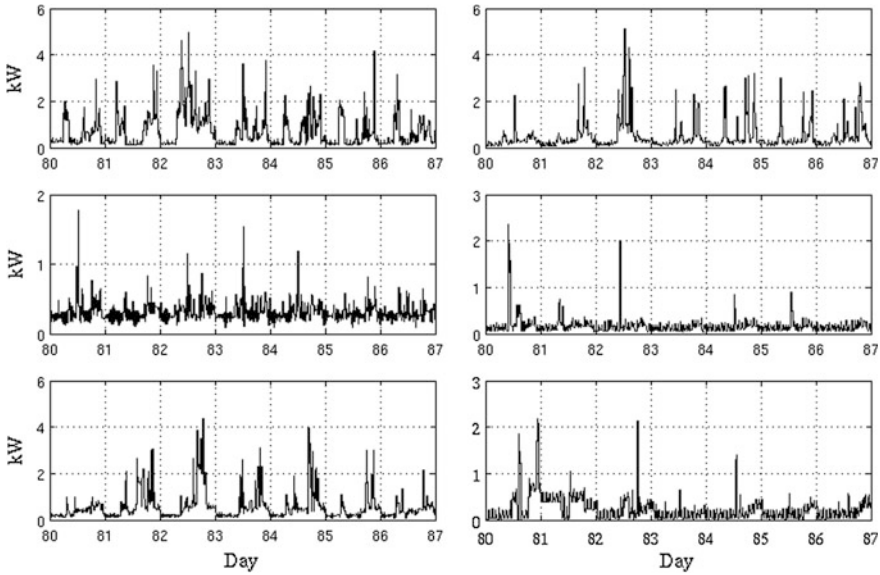
Fig. 6.9 Examples of the household profile data used, for 6 individual households in Belgium, one week starting at day 80 of the year

the roof of households, power quality problems have already started to appear. More information regarding PV and power quality problems in Belgian grids can be found in [22].

Nonetheless, indicative simulations and other work [45, 46] (Chap. 3) suggests that power quality problems in distribution grids due to charging PEVs only comes into view at larger penetration levels of over 30–50 %, and then mostly in weak grids, with unfavorable cable types and lengths. Since we want to study the interference between technical and market level objectives, the focus in the next sections will be on specific cases that represent constrained grids, and not on some average grid situation (if that even exists).

6.4.5.1 Base Physical Grid Structure

Figure 6.10 shows the base topology used in the simulations. A 400 kVA transformer supplies several parallel feeders. Each feeder then supplies a number of household loads, bringing the equivalent transformer load up to 191 households. This is within the limits of the DSO; in a document published by the VREG [47], a maximum occurrence of 220 connections per transformer cabin can be derived. Unfortunately, there is no mention of the rating of the corresponding transformer. The resulting topology is similar to the urban setting used by [45], also with a PEV penetration level of 100 %, but here no PV installations are added, since it was found that they do not cause major changes in the occurrence of undervoltages due
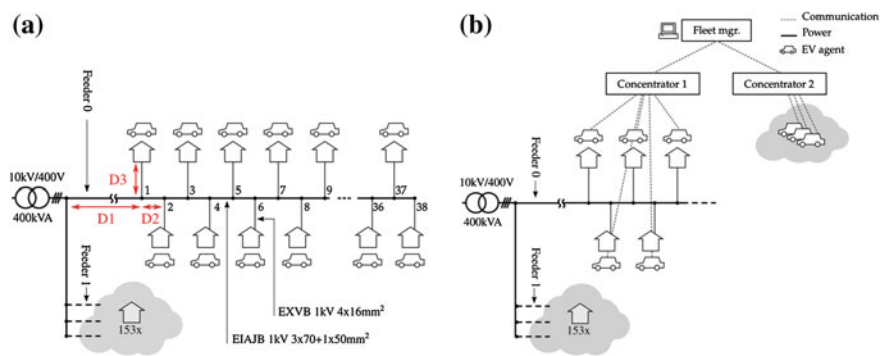
Fig. 6.10 *Left* single instance of the physical grid topology. *Right* agent topology in relation to the physical grid in the single aggregator scenario

to charging. This can be attributed to the non-coincidence of PV production and PEV availability.

One of the feeders, Feeder0, is linked to a line-segment supplying 38 single-phase household connections. These are alternatingly attached to phases 1 to 3 and spaced apart by distance D2. The distance from the transformer to the first household connection is D1. From each connection point, a cable with length D3 runs from the line to the household's supply terminals. In the simulated model, the other feeders and loads (153 households) connected to the transformer are lumped together into one single entity (Feeder 1), as their impact is not studied in detail.

Cable parameters are taken from the design specifications of the standard for underground distribution cables, NBN C33-322 [48]. Cable type EIAJB 1 kV $3 \times 70 + 1 \times 50$ mm^2 is used for the main feeder and line (D1, D2), while cable type EXVB 1 kV 4×16 mm^2 is used to connect the household's supply terminals to the main cable (D3).

Table 6.1 shows the variations on this topology that are evaluated in the next sections. Case NS and NL have a relatively short cable between the transformer and the first household terminal (100 m). Case NL and FL represent scenarios with rather long total cable lengths (914 and 805 m), due to longer distances between the household connection points.

Table 6.1 Variations of the physical base topology, representing various weak grids

Case name	Abbreviation	D1 (m)	D2 (m)	D3 (m)	Total length (m)
NearTransf **S**hortCable	NS	100	15	20	655
NearTransf **L**ongCable	NL	100	22	20	914
FarTransf **S**hortCable	FS	250	7	20	509
FarTransf **L**ongCable	FL	250	15	20	805

Table 6.2 Variations of the agent topology, representing different amounts of vehicles situated in weak grids

Case name	EVs inside weak grid
x-38	38
x-114	3×38
x-380	10×38
x-760	20×38

6.4.5.2 Agent Structure

The organization of the software agents that represent the charging vehicles is independent of the grid topology from the previous section. But, in our simulations, it is assumed that all agents for vehicles that are physically connected to the same transformer are grouped under a single concentrator agent.

At the same time, for the market operation at the fleet manager to function properly, more flexibility than what is provided by the 38 vehicles in the base topology should be available in the cluster. To that end, the cluster is extended so that, depending on the scenario, a total of 200 or 1,000 vehicle agents takes part in the coordinated charging. These additional agents are not part of the load flow calculations. The right side of Fig. 6.8 shows the resulting agent topology.

To test additional shares of PEVs inside weak distribution grids, additional variations of the agent structure are created by having multiples of the base topology. These are shown in Table 6.2. The suffix after the case number determines the share of agents used in the topology.

6.5 Single Aggregator Simulations and Results

In this section, the effect of coordinated charging using market-level objectives on local grid congestion, in the distribution grid scenarios from Sect. 6.4.5, will be examined.

Besides the MAS MBC event-based implementation that was outlined before, we will also include an uncoordinated or dumb charging scenario, during which vehicles plug in and start charging upon arrival at their maximum rated power P_{max}.

6.5.1 Aggregator with ToU Cost Objective

The objective of the fleet manager during a ToU scenario is to respond on a 24-hour horizon ToU tariff in such a way as to minimize the charging cost of the vehicle fleet. The 24-hour tariff is based on the wholesale energy price of the hourly BELPEX day-ahead market. It should be noted that using the price profile of a day-ahead market is not fully representative of a future ToU tariff as it could be implemented by utilities. Still, prices on the day-ahead market do reflect real-world

peak and off-peak periods on an hourly basis, which is what is needed in these simulations.

Because of the seasonal effects of household consumption and tariffs, distribution grid problems are correlated to the time of the year. To limit the influence of the choice of day on the results and get a global picture, randomized sets of scenario parameters are generated and tested. The randomized parameters consist of the day of the year for the tariff, vehicle driving profiles and household load profiles.

The result of 100 randomized parameter sets for each case and coordination option regarding voltage problems according to the EN 50160 standard are shown in Fig. 6.11.

6.5.1.1 Real-Time Level Results

Looking at the household-only (HHOnly) results of Fig. 6.11 indicates that the chosen topologies are sufficient as long as no PEVs are introduced, although voltage regularly fluctuated within the EN50160 specifications. With charging PEVs, the voltage problems are outside the EN 50160 specifications by a wide margin, confirming that the grid topologies qualify as 'weak grid'. Voltages regularly drop below 0.9 pu for more than 5 % of the time, and events where the voltage drops below 0.85 pu are quite common. The problems will no doubt turn for the worse in situations with unbalanced phase connections, higher charge currents (such as future 6.6 kW chargers) and increasing household loads.

Still, the severity of distribution grid problems strongly depends on the grid topology, shown as cases NS, NL, FS and FL. Having the longest cable sections to the loads, case FL leads to the highest amount of voltage magnitude and VUF problems, while case NS and FS experience the least problems.

However, the observed trend is the same: uncoordinated charging is responsible for a peak in the evening that overlaps with the peak of household loads. Charging coordination based on ToU cost minimization objectives leads to only a little less voltage problems. The reason is that, while the coincidence of household loads and charging has disappeared, all available vehicles are now asked to commence charging at one or two points during the day. This creates a new peak that is in itself sufficient to create voltage problems.

To illustrate, Fig. 6.12 shows the power through the feeder and the voltage profile at the worst node for one specific simulated week inside case FL-38, for the event-driven MAS MBC implementation. The situation has the potential to be a lot worse, were the low wholesale prices to correspond to the household evening peak.

It is also immediately visible that the severity of voltage deviations for the implementation with voltage droop controllers is reduced. However, because the voltage droop control only activates below 0.9 pu, the measured values for 0.9 pu deviations are still often outside the 5 % specifications of the EN 50160 standard. Looking at the 0.85 pu results reveals that such occurrences are entirely solved by the use of the voltage droop controller. By tuning the setpoints of the controller so
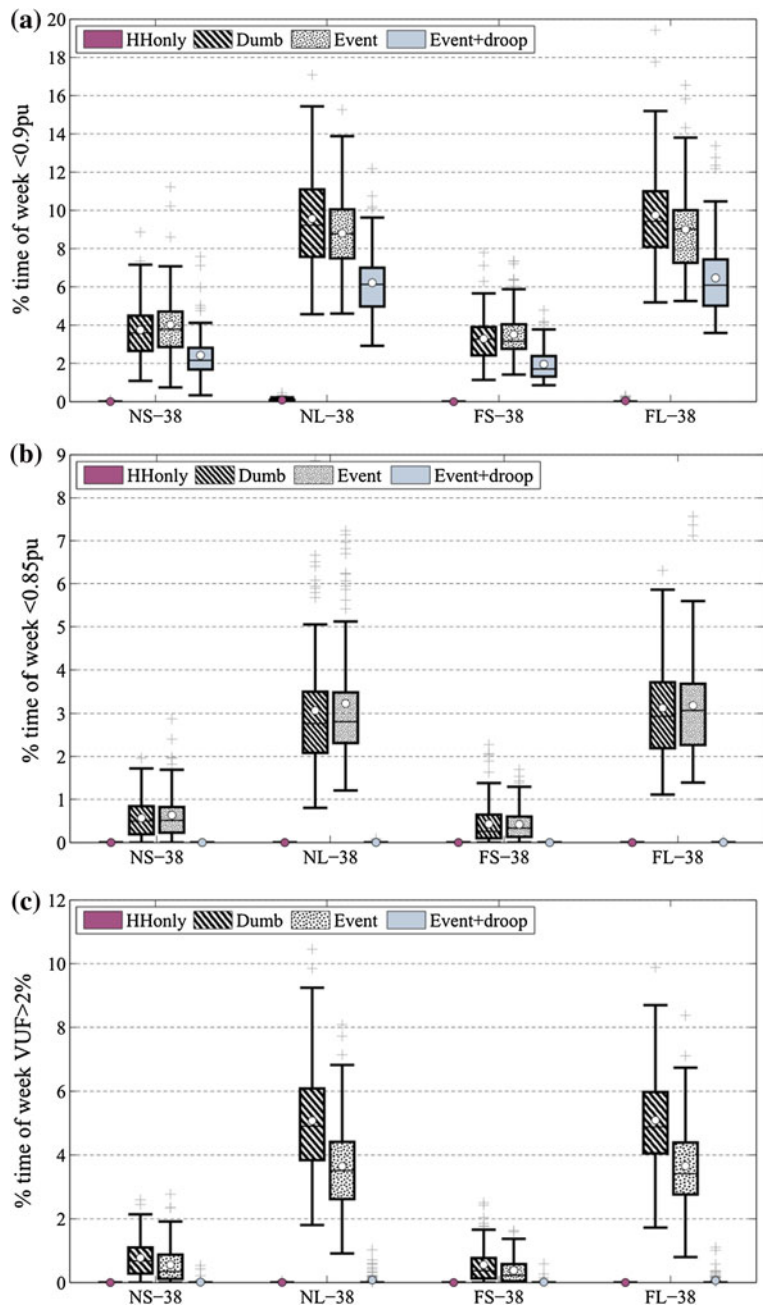
Fig. 6.11 EN 50160 voltage magnitude and unbalance problems, over the course of 7 days, for 100 randomized days
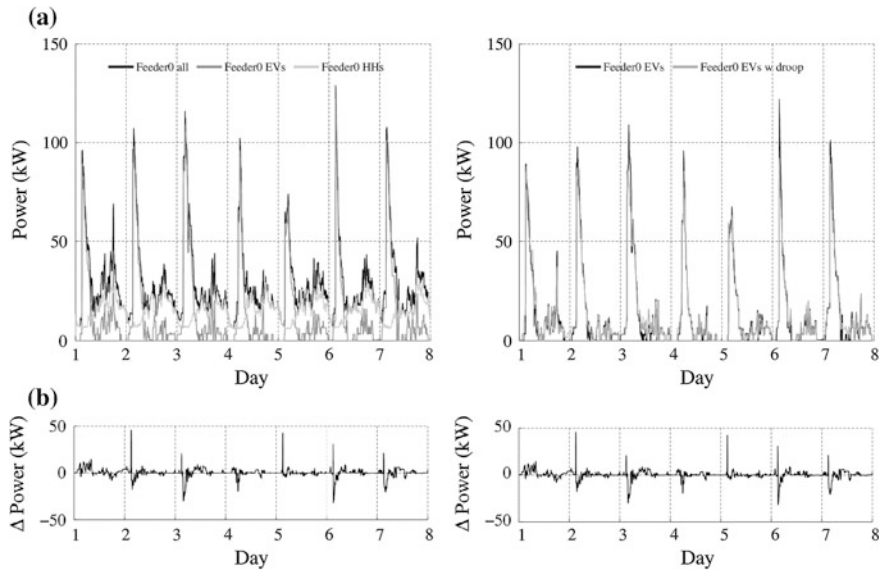
(a)

(b)

Fig. 6.12 Single simulation instance of case FL-38, for the event-based MAS MBC algorithm, week starting at day 16; **a** power profiles, **b** difference between (non)-droop enabled chargers, **c** voltages in the 3 phases of the Feeder0-line and **d** tariff used for ToU objective
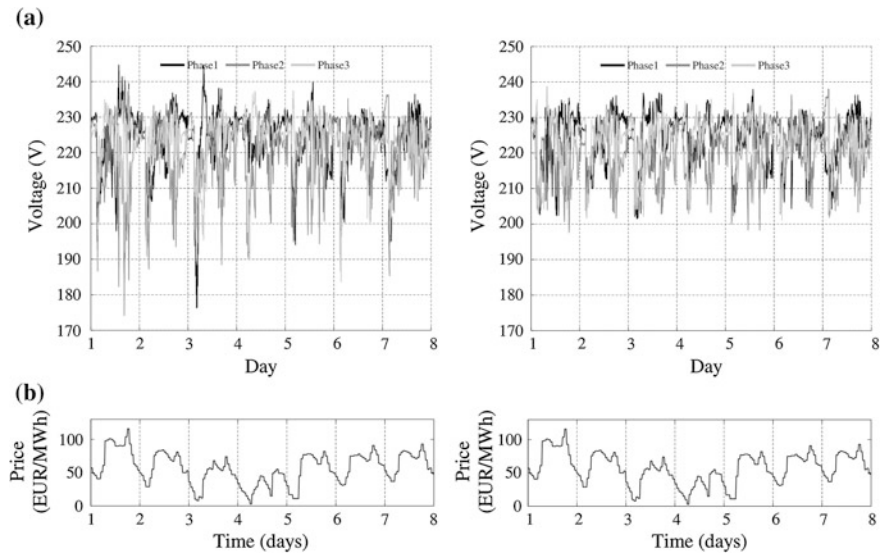
(a)

(b)

Fig. 6.12 (continued)

that it intervenes sooner, the weak grids can be brought into full EN 50160 compliance.

The difference between the power profiles for the case with and without voltage droop controller is also shown in Fig. 6.12. It is visible that, initially, power during the peak is lower, but immediately afterwards part of the 'lost' energy is recovered.

6.5.1.2 Market-Level Results

Table 6.3 shows the cost of charging for a cluster of 200 PEVs. Due to technical constraints, the 8 cases were simulated in separate batches. Because different random parameter sets were generated for each batch, the total cost values between the cases cannot simply be compared.

During droop control intervention, some vehicles can end up with an incompletely charged battery at departure time t_{dep}. Since this influences the cost numbers, a cost has to be attached to the resulting *energy deficit*. E_{deficit} equals the difference between the requested battery level and the level by which the vehicle departed:

$$E_{\text{deficit}} = \sum_i \left(\sum_i {}^i E_{\text{req},t} - {}^i E_{\text{batt},t} | t = {}^i t_{\text{dep}} \right) \tag{6.10}$$

A cost of €50/MWh is assigned to this energy deficit. Of course, the amount of deficit is directly related to the amount of vehicles that can suffer from distribution grid problems. Vehicles outside of weak distribution grids will obviously never end up with lost energy.

Table 6.3 Cost results for the ToU scenarios, and the difference due to the use of voltage droop control in the PEV chargers

Case name	Dumb	Event MBC	Event MBC + droop		Cost diff. due to V droop (%)
			w/o E_{deficit}	w. E_{deficit}	
NS-38	€805.46	€595.00	€596.71	€598.03	+0.28
NL-38	€795.83	€589.72	€594.25	€600.02	+0.77
FS-38	€814.26	€604.59	€606.71	€608.20	+0.35
FL-38	€806.75	€603.77	€609.84	€616.50	+1.00
NS-114	€792.28	€580.16	€585.32	€589.99	+0.89
NL-114	€823.00	€611.03	€626.54	€645.26	+2.50
FS-114	€816.26	€614.34	€620.61	€625.55	+1.02
FL-114	€819.28	€610.95	€630.91	€653.93	+3.27

The cost difference due to the undelivered energy is also shown

While the droop controller has a positive effect on the occurrence of voltage problems, it also increases the cost of charging the fleet, as more energy is consumed during unfavorable periods. Without taking into account the energy deficit at departure time, there is already a small cost increase of 0.6 % for the a-cases, and almost 2 % for the b-cases, where close to 60 % of the PEVs are situated in weak distribution grids. Taking into account E_{deficit}, this cost increase is doubled, and the cumulative battery deficit volume takes up to 1.15 % of the total delivered energy.

6.5.1.3 Conclusions on the ToU Scenario

From the results, it is apparent that *ToU* based controlled charging of PEVs has the potential to create significant power quality problems, because of the tendency to synchronously switch a large amount of the controlled loads when market prices are low, thereby creating large power peaks.

The effect on the state of the distribution grid can be even worse than when no coordinated charging is used (dumb charging). In fact, there were two mitigating factors in the simulations; the household connection points' phases were alternatingly distributed along the line and the price profiles used by the aggregator kept the power peak of the vehicles out of the household's evening peak. If the latter two were not the case, the EN 50160 results would be even worse.

One could argue that, once the penetration level of PEVs reaches a significant share, peak periods will be reflected in the ToU prices, which in turn will favor the spreading of charging load. However, problems in distribution grids can arise much earlier, due to clustering effects, meaning we have large penetration levels in a relatively small geographic area due to demographics. Additionally, when the share of variable renewable energy sources increases, the wholesale price will become more decorrelated from the instantaneous load. E.g. when wind or solar generation is peaking, electricity prices could be low even though the distribution grids are experiencing high load. Influencing distribution grid congestion through ToU tariffs will need carefully designed tariffs [49, 50].

On the positive side, the use of a simple voltage droop controller can practically solve the encountered power quality issues and is able to bring relatively weak distribution grids back into EN 50160 compliance, with some tuning. However, the use of a droop controller has a negative impact on the business case of the aggregator, as the cost of charging goes up and a small number of vehicles do not get their required charge at departure time. But quantitatively speaking, the differences only start to become significant (>2 %) when a large share (>50 %) of an aggregator's fleet is situated inside weak grids (Fig. 6.13).
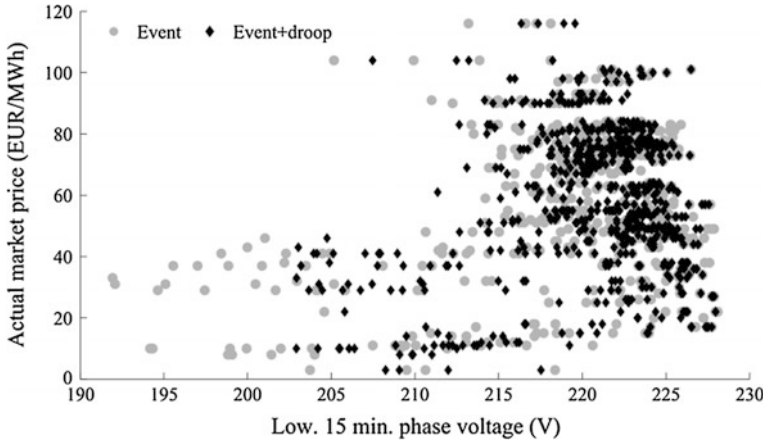
Fig. 6.13 Worst phase voltages observed in Feeder0 versus actual market prices over 7 days, for the MAS MBC algorithm with the ToU-objective, during case FL-38, both active and passive distribution grid. A correlation can be seen between low market prices and the occurrence of low voltages

6.5.2 Aggregator with Balancing Objective

In the previous sections, the objective for the coordinated charging at the market-level has been the cost of charging for the whole fleet. The outcome of an optimization over a *ToU* tariff of the next 24 h and the constraints of the vehicles results in a charging schedule. While a well-established generic objective, it does not entirely represent the potential of coordinated charging for fleet aggregators.

Alternatively, an aggregator could use the flexibility of a fleet to reduce the uncertainty on his portfolio after day-ahead commitments are made, to limit his exposure to the balancing market. In Europe, balancing services are traded on separate markets than wholesale energy [51]. While the prices for these services are correlated to those of the energy markets, they tend to be more expensive. The responsibility and the costs of balancing are usually attributed to an Access Responsible Party (ARP), which will prefer to reschedule their own generation portfolio rather than being exposed to the balancing market.

For wind farms, for example, wind predictions are used to build estimated production profiles and the required day-ahead nominations. Since the predictions are not perfect, real output will deviate from the day-ahead prediction during the day itself, and without intervention this difference leads to a positive or negative imbalance. An example is shown in Fig. 6.14a. By using the energy flexibility of the charging vehicles, an aggregator could try to reduce this wind imbalance.

The main difficulty in compensating for wind prediction errors with PEVs, however, is that large imbalances require the shifting of a considerable share of the fleet's available flexibility. Because the driving behavior of a fleet has a 24 h
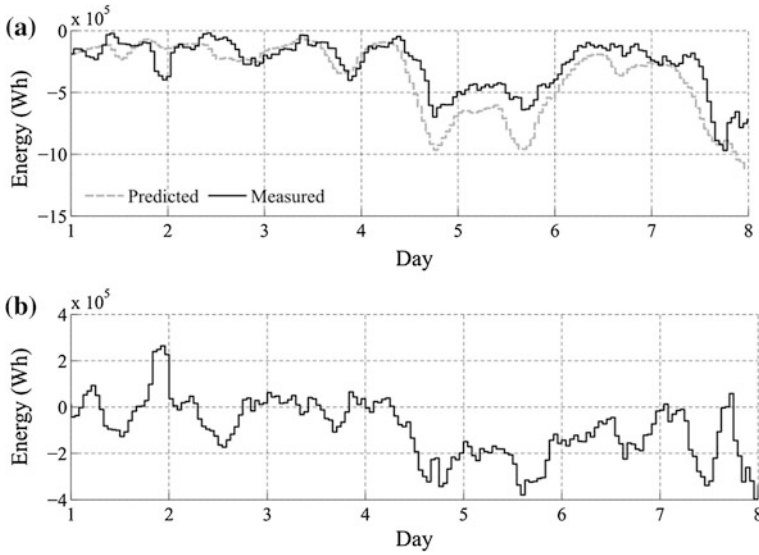
Fig. 6.14 **a** shows predicted and nominated versus measured hourly wind energy for 1.25 MW peak wind power ($W = 0.5$), for one week during March of 2008, and **b** resulting hourly prediction error over the simulated days

periodicity (as seen on Fig. 6.7) and remains relatively constant over time, so is the amount of charging energy per day. At the same time, wind prediction errors do not equal each other out over the course of a day and persist for longer times. Therefore, using all the vehicles' flexibility early in the day means any unexpected imbalance later that day cannot be compensated anymore. A possible solution could consist of incorporating stochastic optimization [52] and intra-day prediction updates to refine the scheduling process.

Another possible source of imbalance lies in the time resolution of the nominations; nominations for the day-ahead market in Belgium require energy values on an hourly basis [53]. However, imbalance volumes are settled on a 15 min basis. Even if an ARP has predictions on his portfolio with high resolution and accuracy, imbalance will still occur as nominated values are averaged per hour.

The description of the optimization problem was already provided in Sect. 6.4.1.

$$E_{\text{opt}} = \underset{E}{\text{argmin}} \sum_{t=0}^{t_{\text{horiz}}} \left(E_{\text{PEV},t} + E_{\text{wind},t} + \frac{1}{4} E_{\text{nomin},t/4} \right)^2 \qquad (6.11)$$

$$E_{\text{nomin},t} = E_{\text{PEV,nomin},t} + E_{\text{wind,nomin},t} \qquad (6.12)$$

The nominated energy E_{nomin} consists of a nomination for the PEV fleet and the day-ahead wind power prediction with a resolution of 1 h, for 24 h. Such nominations have to be determined by the ARP or aggregator, for example from
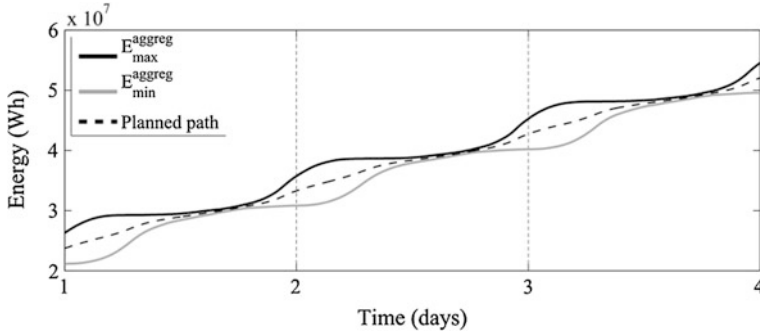
Fig. 6.15 Example PEV nominated energy based on historic aggregated energy constraints data

historical records or estimates. Because the driving behavior of an entire fleet behaves stable and predictable over time, it can be justified to use the power profile of a previous day or week as nomination for the fleet.

When historic energy constraints graphs are used, the amount of flexibility at any given time can be maximized by following an energy path through it according to a fixed ratio of e.g. 1/2 or 1/3 in between E_{max}^{aggreg} and E_{min}^{aggreg}. Figure 6.15 illustrates such a planned path. The power values that correspond to the path can then be translated to hourly energy values to compose $E_{PEV,nomin,t}$.

An extra decay-term, γ can be added to reduce the influence of long-term information in the objective function.

$$E_{opt} = \underset{E}{\arg\min} \sum_{t=0}^{t_{horiz}} \gamma^{t/t_{horiz}} \left(E_{PEV,t} + E_{wind,t} + \frac{1}{4} E_{nomin,t/4} \right)^2 \qquad (6.13)$$

A $\gamma < 1$ will assign a higher optimization cost to the quarter hour imbalance values that are closest in time. In the limit, a $\gamma \to 0$ will mean that the system will act *myopic*, as no information on the future is taken into account. It behaves as the MAS MBC algorithm without planning and minimize instantaneous imbalance.

In order to evaluate the benefit of using this objective, a new 'dumb' scenario is added during which the fleet manager only tries to keep the energy consumption as close as possible to the nomination (referred to as *tracking* the nomination with the fleet). All scenarios use the event-based MAS MBC system to coordinate the fleet, but in the 'tracking' scenario, no optimization to minimize the difference with the nomination using short-term wind data takes place.

6.5.2.1 Simulation Scenarios and Performance Metrics

Due to the relatively long simulation times, the need to prepare nomination data for the wind and PEVs and an exponentially increasing set of parameters, a fixed simulation case is chosen for the simulations, in which the wind and vehicle profiles

start at day 112 of the year. This was chosen because the first 3 days of the consequent week had relatively little wind imbalance and the last 3 relatively large. To end up with a significant amount of energy flexibility, the PEV cluster consists of 1,000 vehicles, instead of 200 for the previous case. Similar to the ToU scenarios, different shares of vehicles can be inside weak distribution grids, according to Table 6.2.

The main performance indicator consists of the total energy volume of remaining quarter hourly imbalance and the resulting cost. For the latter, real market data on the positive and negative imbalance price from the Transmission System Operator (TSO) Elia is used. It should be noted that the price data used dates from 2012, because the operating principle of the imbalance settlement was changed from then onwards, while the wind data available is from 2008.

While the total remaining imbalance volume accumulated during a simulation gives a good idea about the performance, it does not tell anything about its distribution during the day. From Fig. 6.14a, it can be seen that during the first 3 days, nominated and measured wind energy values are reasonably balanced over the course of a day. However, during the last 4 days, the difference between prediction and measured energy exists for the whole period. This is apparent from Fig. 6.14b, where the resulting prediction error during each hour of the simulation is shown. Unless the ratio of energy flexibility to wind power is very high, it is difficult to end up without imbalance under such conditions.

But the quadratic nature of the objective will favor to spread out imbalance as much as possible, so that a relatively flat imbalance profile should be obtained in the case of $\gamma = 1$. Therefore, looking solely at the remaining imbalance volume as a measure of performance would not capture the intent of the algorithm's objective. In fact, a myopic algorithm, instantly matching imbalance figures with the flexibility of PEVs, will perform better regarding the remaining imbalance volume.

Because the ability to smoothen or influence the occurrence of imbalance can be very beneficial for an ARP, it makes sense to look at the "variability" of the imbalance profiles. The spectral content of the imbalance profile is obtained by taking the sum of FFTs over a sliding window of 32 profile samples. Then the mean value is subtracted to get rid of the DC component, and the surface under the spectral plot is kept, expressed in kW Hz. The higher this value, the more variability there is on the remaining imbalance's power profile.

To evaluate the effects at the real-time level, the EN 50160 specifications and performance indicators from the ToU case, are used here as well.

6.5.2.2 Market-Level Results

In a first simulation, only the behavior at the market level is investigated, disregarding the distribution grid completely. In Fig. 6.16a, the 15 min imbalance volumes are plotted for different values of γ, for a simulation covering the 7 days from Fig. 6.14. It is visible that the event-based balancing successfully reduces the amount of imbalance with the nomination. Smaller γ values lead to aforementioned
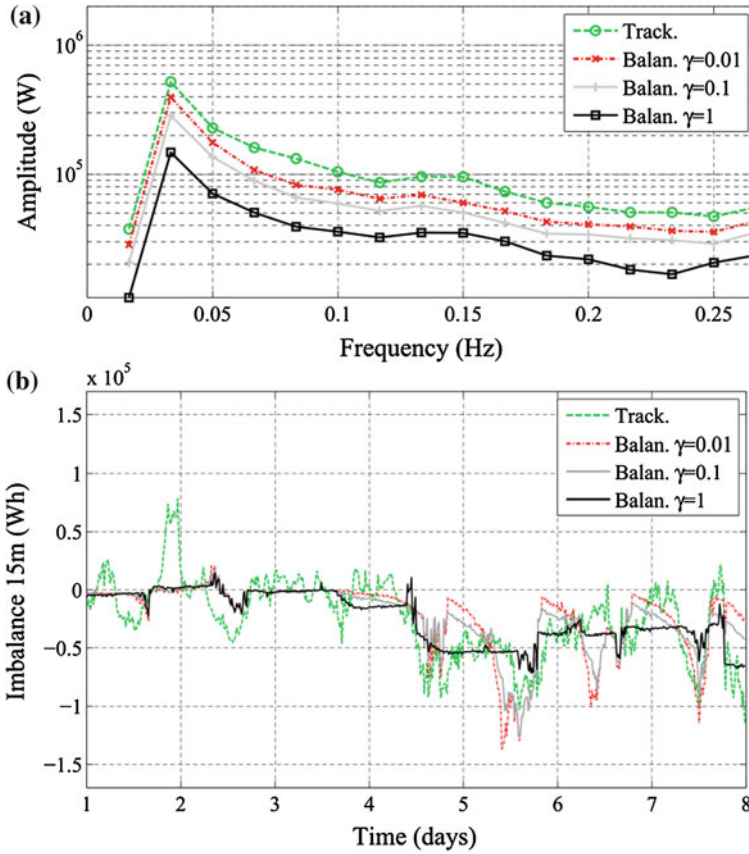
Fig. 6.16 Imbalance scenario, **a** remaining imbalance profile for different values of γ over the course of 7 days and for a peak wind output of 1.25 MW (W = 0.5), together with the tracking scenario and **b** spectral plot of the power profiles expresses variability of the remaining imbalance

'myopic' behavior and force the imbalance profile close to zero, until of course the aggregator runs out of short-term flexibility.

In Fig. 6.16b, the Fourier transformed imbalance volume is plotted. This figure thus shows its frequency components. In case of the balancing optimization scenarios, it is visible that their imbalance profiles contain less high-frequency components then when no balancing optimization is done. This confirms what can be seen in Fig. 6.16a, namely that the case with the balancing optimization for $\gamma = 1$. is able to better spread out the remaining imbalance.

In the above scenario, the wind nominations and measurements were scaled with a factor $W = 0.5$, to obtain a peak wind output of 1.25 MW. Varying ratios of wind and vehicles have also been examined, of which the results are shown in Table 6.4.

The improvement in remaining imbalance volume over the tracking case is between 20 and 30 %. Smaller γ values lead to slightly less remaining imbalance

Table 6.4 Balancing case simulation results for 7 consecutive days and a cluster 1,000 PEVs, for different values of the wind scaling parameter W and discount factor γ

W = 0.05 (0.125 MWp)	Imbal Volume (MWh)	Imbal Cost	Volume diff. (%)	Spectr. (kW Hz)	Spectr. diff (%)
Tracking nomin.	2.543	€171.2	0	2.7	0
Balancing $\gamma = 1$	2.087	€128.7	−17.9	2.5	−7.4
Balancing $\gamma = 0.1$	1.988	€120.9	−21.8	3.1	+14.8
Balancing $\gamma = 0.01$	1.967	€117.1	22.7	3.5	+29.6
W = 0.2 (0.5 MWp)					
Tracking nomin.	8.633	€580.3	0	9.3	0
Balancing $\gamma = 1$	6.832	€434.3	−20.7	3.3	−64.5
Balancing $\gamma = 0.1$	6.322	€397.8	−26.8	6.2	−33.3
Balancing $\gamma = 0.01$	6.131	€379.7	−28.9	8.0	−14.0
W = 0.5 (1.25 MWp)					
Tracking nomin.	21.056	€1413	0	23.2	0
Balancing $\gamma = 1$	16.680	€1091	−20.8	7.6	−67.2
Balancing $\gamma = 0.1$	15.775	€1014	−25.1	13.2	−43.1
Balancing $\gamma = 0.01$	15.313	€989.4	−27.3	16.9	−27.2
W = 0.7 (1.75 MWp)					
Tracking nomin.	29.364	€1970	0	32.5	0
Balancing $\gamma = 1$	23.888	€1570	−18.6	12.2	−62.5
Balancing $\gamma = 0.1$	22.860	€1471	−22.1	18.9	−41.2
Balancing $\gamma = 0.01$	22.216	€1443	−24.3	23.8	−23.8
W = 1.0 (2.5 MWp)					
Tracking nomin.	41.830	€2806	0	46.4	0
Balancing $\gamma = 1$	35.112	€2324	−16.1	20.8	−55.2
Balancing $\gamma = 0.1$	33.762	€2186	−19.3	29.2	−37.1
Balancing $\gamma = 0.01$	33.141	€2150	−20.8	34.9	−24.8

over 7 days compared to $\gamma = 1$. However, since the objective of the optimization is related to the quadratic imbalance over the optimization horizon, the conclusion that a myopic algorithm performs better based on the total remaining imbalance would be misleading. It has to be looked at together with the 'spreading' of the remaining imbalance, expressed by the spectral content on the 'Volume difference' column of Table 6.4.

For larger wind scaling factors and thus larger wind prediction error volumes, the improvement regarding remaining imbalance decreases to 16–21 %. A similar effect is observed for the spectral content values. It can be deduced that, based on this balancing method, around 1–1.25 MW of wind power can be properly compensated per 1,000 PEVs. Higher or lower shares of wind power decrease the efficiency of this system.

6.5.2.3 Real-Time Level Results

For the effects at the distribution level, the different cases and its variations again come into play. From the tested parameters in the previous section, we keep the wind scaling of $W = 0.5$, since this parameter led to the best performance at the market level, and a γ of 1, as this is the most generic application.

The EN 50160 results of the passive distribution grid scenarios are grouped together with the active distribution grid scenarios in Fig. 6.17, to improve clarity and avoid duplication. These plots show the results for the FL case, but the household-only results have been omitted, since their results are the same as in the previous section.

Fig. 6.17 EN 50160 voltage magnitude stats for the single-aggregator balancing scenarios; **a** V < 0.9 pu, **b** V < 0.85 pu and (**c**) VUF > 2 %
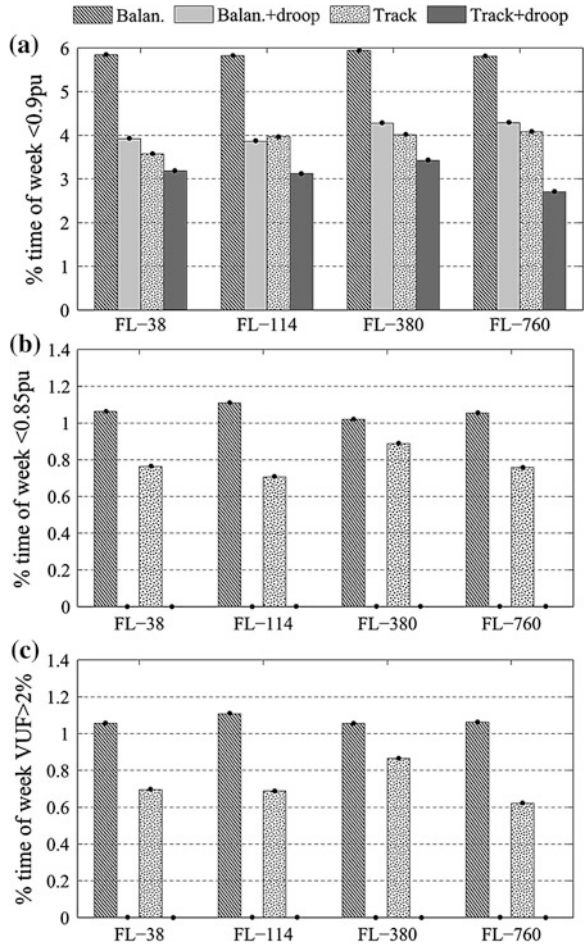
Compared to the ToU results, problems are a lot less worse, but voltages still drop below 0.85 pu. The use of voltage droop control reduces the limited remaining voltage problems to below the EN 50160 specifications.

Since the tracking scenario already tries to follow the nomination, which is a smooth path through the aggregated energy constraints graph for the PEVs, the reduction in voltage deviations are relatively small when voltage droop controllers are introduced, in comparison to the balancing case.

6.5.2.4 Impact of Droop Control on Market-Level Objectives

The amount of vehicles that is affected by voltage droop activation is expected to influence the business case at the market level. It would follow that moving from case FL-38 to FL-760 will increase the remaining imbalance, as less and less peak flexibility is available to the fleet manager. Figure 6.18 shows that the imbalance volume is constant for case FL-38 and FL-114, having respectively 4 and 21 % of all the PEVs inside of a weak grid.

For case FL-380, with 38 % of the fleet inside the weak distribution grids, a small increase of 2.4 % in the imbalance volume is noticeable, and finally, for the case FL-760 with 76 % of the PEVs located inside the constrained grids, the observed increase in imbalance volume is 10.3 %. During the latter, the 'dumb' tracking scenario also suffered slightly with a minor 0.95 % increase.

6.5.2.5 Conclusions on the Balancing Case

The balancing concept was successfully tested on a portfolio consisting of wind generation and charging PEV's. The optimization reduces both the imbalance that
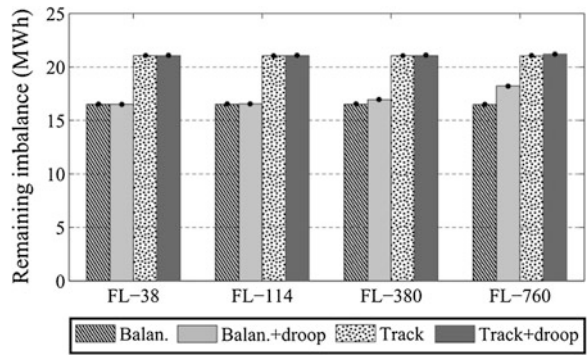

Fig. 6.18 Total remaining imbalance after 7 days, for different shares of PEVs in weak distribution grids. At larger shares, an effect on the remaining imbalance is noticeable, as the aggregator fails to compensate for the activation of the droop controllers

originates from the hourly discretization of the day-ahead nomination, and the imbalance that exists because of imperfect wind speed predictions. Using short-term information on the wind production, the imbalance can also be intentionally spread in time. This can be beneficial for the aggregator, as the remaining imbalance could then be countered by other generation units in its portfolio.

Additionally, the effect of varying the discount factor γ was shown. By including γ as variable into the optimization, one could move the remaining imbalance towards points in time where this has economical benefits, such as by using stochastic information on the imbalance market prices.

Regarding grid constraints, the use of the (quadratic) balancing objective puts less load on the grid compared to the (linear) ToU objective, because flexibility of the PEVs is intentionally spread out when creating the nomination of the charging energy and therefore not enabled all at once.

As in the ToU case, voltage droop controllers inside PEV chargers are successful in mitigating weak grid constraints. Some tuning of its parameters may be needed to find a setting where the grid state at all nodes is within the EN 50160 specifications during all the time.

Unless a very large share of PEVs of a coordinated charging fleet manager is located inside weak grids, the business case is practically unaffected by the addition of local voltage droop control, using the coordination system that was implemented in this work. That means being event-based for fast response and having a compensation loop at the fleet manager. The combination of both ensures that, when droop controllers activate, the equilibrium priority is changed quickly enough so that the flexibility of other vehicles is dispatched to compensate for the 'loss' in expected energy over time.

6.6 Multi-aggregator Simulations and Results

In many cases, when studying coordinated charging of PEVs, there is only a single fleet manager or aggregator. However, if the business case of using the energy flexibility of vehicles takes off, it can be anticipated that multiple competing services will become available. This leads to the question what problems can arise if multiple aggregators are active within the same distribution grid, as illustrated by Fig. 6.19.

In case of problems, is there a need for additional congestion management mechanisms, to ensure that capacity inside individual grids is allocated to the aggregator's objective that has the highest value, or is the use of a voltage droop controller that intervenes when problems arise sufficient?

The advantage of a voltage droop controller lies in its simplicity of operation and the fact that it does not rely on communication with external actors. More complex grid congestion management systems, briefly touched upon in Sect. 6.2.2.2, assign
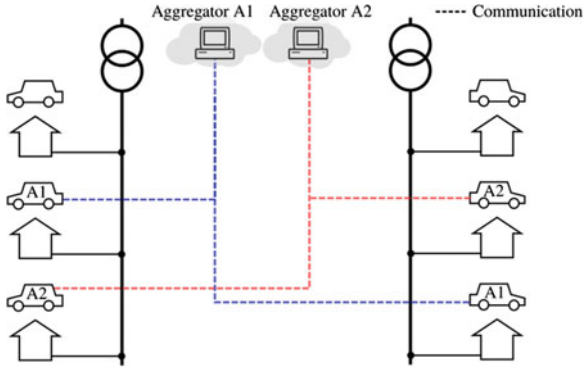
Fig. 6.19 Multi-aggregator grid situation. Two aggregators, A1 and A2, control a number of charging EVs that are connected to the same distribution grid transformer

an active role to the DSO, that must perform ahead-of-time capacity allocation and/ or check iteratively whether all aggregators' schedules are feasible (advance capacity allocation). This would be required for every grid segment wherein aggregators are active. Or, a DSO could set up dynamic ToU network tariffs based on location and projected network load.

6.6.1 Aggregators with ToU Cost Objective

Since the use of a ToU objective implies that aggregators use the same actual market prices, a multi-aggregator version of the ToU scenario of Sect. 6.5.1 does not perform any different than its single-aggregator counterpart. Therefore, the simulations and results have been omitted.

However, in case one aggregator is serving mostly customers that are located at the beginning of a line and the other aggregator mainly ones at the end, the latter will be at a disadvantage. A similar situation will occur if the phase connections are heavily correlated with the aggregator assignment.

6.6.2 Aggregators with Balancing Objective

During the balancing case, different aggregators can base their optimizations on different predictions or portfolios, and the expected results are not as straightforward to derive as in the ToU cases.

In the simulations, both aggregators will be using an identical portfolio, again consisting of a fleet of 1,000 PEVs combined with 1.25 MW of peak wind generation. To have a realistic case that represents wind generation in a geographically shared region, the wind predictions should at least be correlated, which is taken care of by adding one day of difference for the second aggregator.

To ensure that aggregators each have the same fleet size, the total amount of vehicles in the simulations has to be doubled. Again, different cases represent varying shares of vehicles that are inside the weak distribution grids. Case FL-38 has been left out, since at less than 4 % of PEVs inside a weak grid, the effects during the balancing scenario are practically zero, as previously shown.

6.6.2.1 Real-Time Level Results

On Fig. 6.20, the EN 50160 results are plotted for cases x-114, x-380 and x-760 (respectively with 114,380 and 760 of 1,000 PEVs inside weak distribution grids). Compared to the single-aggregator scenario, the severity of the voltage deviations is a lot less. This can be entirely attributed to the reduced coincidence of the objectives of both aggregators.

6.6.2.2 Market Level Results

The total remaining imbalance for both aggregators after one simulated week is shown in Fig. 6.21. Just as with the single aggregator case in Fig. 6.18, the imbalance volume is only affected by the droop controllers at high shares of PEVs in weak grids. The absolute volume of aggregator A2 is lower because its wind profile starts one day earlier than that of A1, thereby avoiding a day with large prediction error.

6.6.2.3 Conclusions on the Multi-aggregator Case

From the results, it can be concluded that settings where two aggregators are active within the same part of the distribution grid do not show problematic behavior. This is due to the fact that the wind profiles are not the same for both aggregators, so that access to PEVs' flexibility in one distribution grid is spread out and less voltage deviations appear. Therefore, in the worst case, voltage deviations would be similar to those of the single-aggregator case.

With these results in mind, and based on the implemented DR algorithm with voltage droop controllers inside the presented grid configurations, the necessity of additional grid congestion management mechanisms can be questioned. The

Fig. 6.20 EN 50160 voltage
magnitude stats for the multi-
aggregator balancing
scenarios; **a** V < 0.9 pu,
b V < 0.85 pu and
c VUF > 2 %
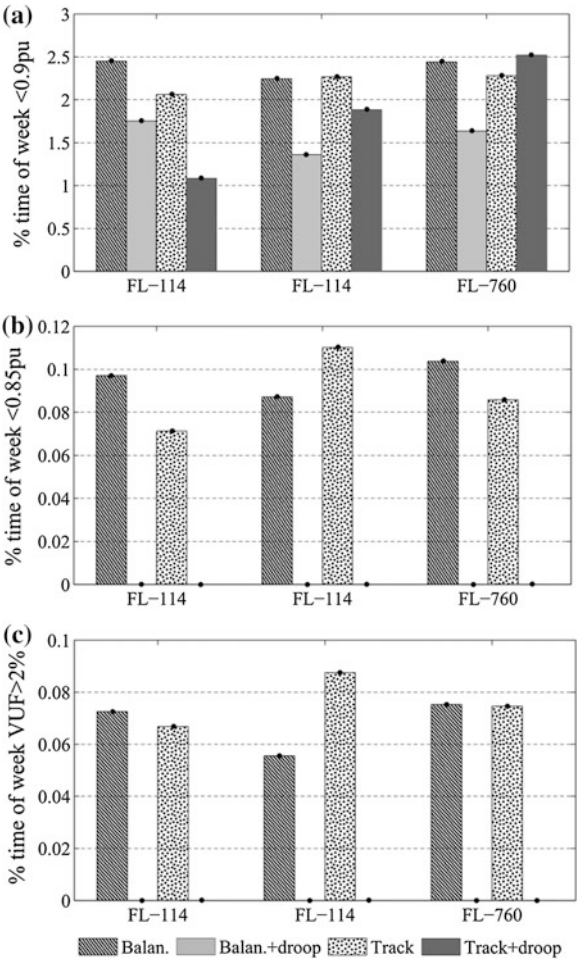
complexity introduced by such solutions, computationally and from a responsibility
perspective, are hard to justify with the amount of gains that can be achieved.

It was however assumed that the PEVs were evenly assigned to both aggrega-
tors. In the situation where one aggregator controls all the PEVs at the beginning of
a grid and the other all the PEVs towards the end of the line, the latter will be
subjected to more droop activations and be at a disadvantage compared to the other
aggregator. But again, the limited energy deficits this causes might not warrant the
deployment of grid congestion management mechanisms (e.g. capacity markets in
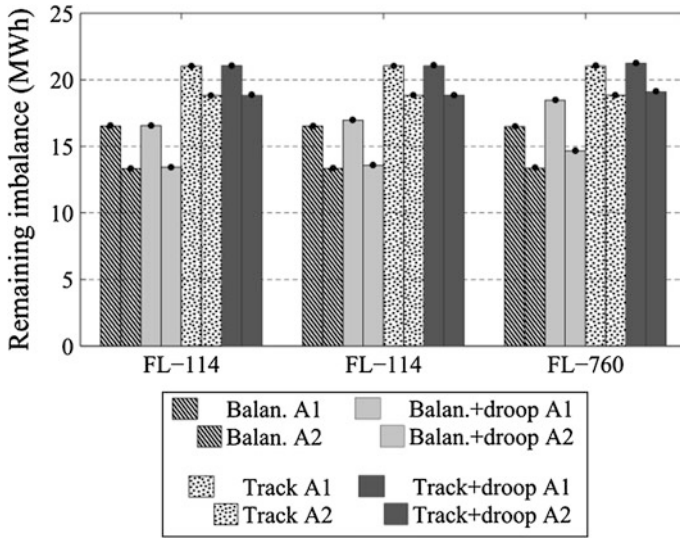cooperation with the DSO, Sect. 6.2.2.2).

Fig. 6.21 Total remaining imbalance after 7 days. *Left side* of the bar represents aggregator A1, *right side* aggregator A2

6.7 Conclusions

In the light of the challenges that were discussed in the introduction, we can summarize the results and contributions as follows:

- The separation between two demand response operation levels was identified; the market operation level is responsible for the business case of a fleet of PEVs and operates synchronous with the energy markets. The technical or real-time operation level uses the setpoints determined by the business case and uses an event-driven architecture to efficiently dispatch constraints from and control signals to the charging PEVs. At the market level, an algorithm based on MBC was adapted for the coordination of PEVs, and at the technical level, a voltage droop controller is integrated to be able to respect the local grid constraints.
- The effect of using market-level objectives on congestion in weak distribution grids has been examined. Especially the use of ToU cost minimization objectives has a negative effect on the occurrence of undervoltages, with respect to the EN 50160 standard. Synchronization of large amounts of controllable loads is to be avoided in DR.
- Besides a ToU cost minimization objective, it has been shown that a cluster of fast-responding PEVs can be used to limit an aggregator's exposure to the balancing market. An optimization at the market level determines setpoints for the fleet such that the remaining imbalance between predicted and nominated wind output and more recent short-term predictions is spread out in time. This can be beneficial for the aggregator, as the remaining imbalance could be then

be countered by other generation units in its portfolio. Additionally, one could include γ as variable into the optimization to express a preference of having the remaining imbalance occur when this has economical benefits.

- A straightforward and common way of mitigating grid congestion is the use of a voltage droop controller. While fast, inexpensive and able to act independently from any central coordinator, its activation will intervene in the the business case. In literature, the overruling of the market operation level by technical objectives is often presented as a major challenge to be addressed. The results in Sects. 6.5 and 6.6 show that, unless very large shares of the PEV fleet are located inside weak grids, the effects of the activation of voltage droop controllers on the business case remains relatively modest. This is due to the limited amount of scheduled energy that is 'lost' and the possibility to compensate for by other parts in the DR cluster, with the event-driven approach.

- Additionally, situations where multiple aggregators are active within the same distribution grid were also looked at. Based on the assumptions made and using the presented DR algorithm, it can be stated that the use of voltage droop controllers only is already effective in mitigating grid congestion problems without significantly disturbing the aggregators' business case. The need for additional grid congestion management algorithms, e.g. a capacity market in cooperation with the DSO, might better be reserved to a few corner cases where increasing the transfer capacity of the grid is (economically or otherwise) infeasible.

References

1. Geth F, Leemput N, Van Roy J, Buscher J, Ponnette R, Driesen J (2012) Voltage droop charging of electric vehicles in a residential distribution feeder. In: 3rd IEEE PES innovation smart grid technology Europe, (ISGT Europe) IEEE, pp 1–8
2. De Craemer K, Vandael S, Claessens B, Deconinck G (2013) An event-driven dual coordination mechanism for demand side management of PHEVs. IEEE Trans Smart Grid pp 1–10. doi:10.1109/TSG.2013.2272197
3. Clement-Nyns K, Haesen E, Driesen J (2010) The impact of charging plug-in hybrid electric vehicles on a residential distribution grid. IEEE Trans Power Syst 25:371–380. doi:10.1109/TPWRS.2009.2036481
4. Shao S, Pipattanasomporn M, Rahman S (2012) Grid integration of electric vehicles and demand response with customer choice. IEEE Trans Smart Grid 3:543–550. doi:10.1109/TSG.2011.2164949
5. Gatsis N, Giannakis GB (2012) Residential load control: distributed scheduling and convergence with lost AMI messages. IEEE Trans Smart Grid 3:770–786. doi:10.1109/TSG.2011.2176518
6. Gatsis N, Giannakis GB (2011) Cooperative multi-residence demand response scheduling. In: 45th Annual conference on information sciences and systems, IEEE, pp 1–6
7. Fan Z (2012) A distributed demand response algorithm and its application to PHEV charging in smart grids. IEEE Trans Smart Grid 3:1280–1290. doi:10.1109/TSG.2012.2185075
8. Weckx S, Driesen J, D'hulst R (2013) Optimal real-time pricing for unbalanced distribution grids with network constraints. In: IEEE Power and energy society general meeting, IEEE, pp 1–5

9. Ma Z, Callaway D, Hiskens I (2010) Decentralized charging control for large populations of plug-in electric vehicles. 49th IEEE conference on decision and control, IEEE, pp 206–212
10. Anderson RN, Boulanger A, Powell WB, Scott W (2011) Adaptive stochastic control for the smart grid. Proc IEEE 99:1098–1115. doi:10.1109/JPROC.2011.2109671
11. Wong VWS (2011) An approximate dynamic programming approach for coordinated charging control at vehicle-to-grid aggregator. In: International conference on smart grid communications, IEEE, pp 279–284
12. Robu V, Stein S, Gerding E, Parkes D, Rogers A, Jennings N (2012) An online mechanism for multi-speed electric vehicle charging. In: 2nd International conference on auctions, market mechanisms, and their applications. Springer, Heidelberg, pp 100–112
13. Galus MD, La Fauci R, Andersson G (2010) Investigating PHEV wind balancing capabilities using heuristics and model predictive control. In: IEEE power and energy society general meeting, IEEE, pp 1–8
14. Biegel B, Andersen P, Pedersen TS, Nielsen KM, Stoustrup J, Hansen LH (2013) Smart grid dispatch strategy for on/off demand-side devices. Control Conference (ECC), Europe, pp 2541–2548
15. Koch S, Mathieu JL, Callaway DS (2011) Modeling and control of aggregated heterogeneous thermostatically controlled loads for ancillary services. In: Proceedings of 17th Power Systems Computation Conference
16. Vandael S, Claessens B, Hommelberg M, Holvoet T, Deconinck G (2013) A scalable three-step approach for demand side management of plug-in hybrid vehicles. IEEE Trans Smart Grid 4:720–728. doi:10.1109/TSG.2012.2213847
17. Bach Andersen P, Hu J, Heussen K (2012) Coordination strategies for distribution grid congestion management in a multi-actor, multi-objective setting. In: 3rd IEEE PES innovation smart grid technology Europe, (ISGT Europe) IEEE, pp 1–8
18. CENELEC (2010) EN 50160—Voltage characteristics of electricity supplied by public electricity networks, July 2010
19. Pillay P, Manyage M (2001) Definitions of voltage unbalance. IEEE Power Eng Rev 21:50–51. doi:10.1109/39.920965
20. Seljeseth H, Henning T, Solvang T (2013) Measurements of network impact from electric vehicles during slow and fast charging. In: 22nd International Conference on Electricity Distribution
21. Liu MB, Canizares CA, Huang W (2009) Reactive power and voltage control in distribution systems with limited switching operations. IEEE Trans Power Syst 24:889–899. doi:10.1109/TPWRS.2009.2016362
22. Gonzalez C, Geuns J, Weckx S, Wijnhoven T, Vingerhoets P, De Rybel T, Driesen J (2012) LV distribution network feeders in Belgium and power quality issues due to increasing PV penetration levels. In: 3rd IEEE PES innovation smart grid technology Europe, (ISGT Europe) IEEE, pp 1–8
23. Efkarpidis N, Gonzalez C, Wijnhoven T, Van Dommelen D, De Rybel T, Driesen J (2013) Technical assessment of on-load tap-changers in flemish LV distribution grids. International work integrative solar power into power systems
24. Kester CPJ, Heskes JMP, (Sjaak) Kaandorp JJ, (Sjef) Cobben JFG, Schoonenberg G, Malyna D, De Jong ECW, Wargers BJ, (Ton) Dalmeijer AJF (2009) A smart MV/LV-station that improves power quality, reliability and substation load profile. In: 20th International conference on electricity distribution, pp 8–11
25. DIN VDE Std. VDE-AR-N 4105 (2011) Erzeugungsanlagen am Niederspannungsnetz, Technische Mindestanfor-derungen für Anschluss und Parallelbetrieb von Erzeugungsanlagen am Niederspannungsnetz
26. Synergrid C10/11 (2012) Specifieke technische voorschriften voor decentrale productie-installaties die in parallel werken met het distributienet
27. Loix T (2011) Participation of inverter-connected distributed energy resources in grid voltage control. KU Leuven

28. Clement-Nyns K, Haesen E, Driesen J (2011) The impact of vehicle-to-grid on the distribution grid. Electr Power Syst Res 81:185–192. doi:10.1016/j.epsr.2010.08.007

29. Peças Lopes JA, Polenz SA, Moreira CL, Cherkaoui R (2010) Identification of control and management strategies for LV unbalanced microgrids with plugged-in electric vehicles. Electr Power Syst Res 80:898–906. doi:10.1016/j.epsr.2009.12.013

30. Garcia-Valle R, Peças Lopes JA (2013) Electric vehicle integration into modern. Power Netw. doi:10.1007/978-1-4614-0134-6

31. Biegel B, Andersen P, Stoustrup J, Bendtsen JD (2012) Congestion management in a smart grid via shadow prices. In: 8th IFAC symposium on power plant and power system control, pp 518–523

32. Sundstrom O, Binding C (2012) Flexible charging optimization for electric vehicles considering distribution grid constraints. IEEE Trans Smart Grid 3:26–37. doi:10.1109/TSG.2011.2168431

33. O'Connell N, Wu Q, Østergaard J, Nielsen AH, Cha ST, Ding Y (2012) Day-ahead tariffs for the alleviation of distribution grid congestion from electric vehicles. Electr Power Syst Res 92:106–114

34. Verzijlbergh R (2013) The power of electric vehicles—exploring the value of flexible electricity demand in a multi-actor context. Dissertation, TU Delft

35. Kok K (2013) The powermatcher: smart coordination for the smart electricity grid, p 314. Vrije Universiteit, Amsterdam

36. Kok K, Warmer K, Kamphuis R (2005) PowerMatcher: multiagent control in the electricity infrastructure. In: Proceedings of the 4th international joint conference on autonomous agents and multiagent systems (AAMAS 05'). New York, pp 75–82

37. Kok JK, Scheepers MJJ, Kamphuis IG (2010) Intelligence in electricity networks for embedding renewables and distributed generation. Intelligent infrastructures, Springer, pp 179–209

38. Van Roy J, Leemput N, Geth F, Salenbien R, Buscher J, Driesen J (2014) Apartment building electricity system impact of operational electric vehicle charging strategies. IEEE Trans Sustain Energy 5:264–272. doi:10.1109/TSTE.2013.2281463

39. Van Roy J, Leemput N, De Breucker S, Geth F, Peter T, Driesen J (2011) An availability analysis and energy consumption model for a flemish fleet of electric vehicles. European Electrical Vehicle Congr Brussels, p 12

40. Raab AF, Ellingsen M, Walsh A (2011) Mobile energy resources in grids of electricity—WP 1 Task 1.6 Deliverable D1.4—learning from EV FIeld Tests

41. Brand AJ, Kok K (2003) Aanbodvoorspeller duurzame energie. https://www.ecn.nl/avde/

42. Brand AJ (2008) Wind power forecasting method AVDE. China Glob Wind Power

43. Nordex (2009) Datenblatt N80/2500 (2.5 MW). http://www.nordex-online.com/en/produkte-service/wind-turbines/n80-25-mw/product-data-sheet-n80-25mw.html

44. Dupont B, Vingerhoets P, Tant P, Vanthournout K, Cardinaels W, De Rybel T, Peeters E, Belmans R (2012) Linear breakthrough project: large-scale implementation of smart grid technologies in distribution grids. In: 3rd IEEE PES innovation smart grid technology Europe, (ISGT Europe) IEEE, pp 1–8

45. Leemput N, Geth F, Van Roy J, Delnooz A, Büscher J, Driesen J (2014) Impact of electric vehicle on-board single-phase charging strategies on a flemish residential grid. IEEE Trans Smart Grid, 5(4)1815–1822. doi: 10.1109/TSG.2014.2307897

46. Clement-Nyns K (2010) Impact of plug-in hybrid electric vehicles on the electricity system. KU Leuven

47. VREG (2013) RAPP-2013-06—De kwaliteit van de dienstverlening van de elektriciteitsdistributienetbeheerders in het Vlaamse Gewest in 2012

48. NBN (1975) C33-322—Kabels Voor Ondergrondse Aanleg, met Synthetische Isolatie en Versterkte Mantel (Type 1 kV)

49. Shao S, Zhang T, Pipattanasomporn M, Rahman S (2010) Impact of TOU rates on distribution load shapes in a smart grid with PHEV penetration. IEEE PES transmission and distribution, IEEE, pp 1–6

50. Dupont B, De Jonghe C, Olmos L, Belmans R (2014) Demand response with locational dynamic pricing to support the integration of renewables. Energy Policy 67:344–354. doi:10.1016/j.enpol.2013.12.058
51. Baritaud M (2012) Securing power during the transition. Generation investment and operation, IEA (International Energy Agency), pp 47
52. Vaya MG, Andersson G (2013) Integrating renewable energy forecast uncertainty in smart-charging approaches for plug-in electric vehicles. IPowerTech (POWERTECH), 2013 IEEE Grenoble, pp 1–6, IEEE
53. Elia (2014) Nominated capacity: Belgium—Netherlands. http://www.elia.be/en/grid-data/interconnections/nominated-capacity-bel-neth. Accessed 20 Jan 2014